

Multidimensional quantum solitons with nondegenerate parametric interactions: Photonic and Bose-Einstein condensate environments

K. V. Kheruntsyan and P. D. Drummond

Department of Physics, University of Queensland, St. Lucia, QLD 4067, Australia

(Received 3 August 1999; published 17 May 2000)

We consider the quantum theory of three fields interacting via parametric and repulsive quartic couplings. This can be applied to treat photonic $\chi^{(2)}$ and $\chi^{(3)}$ interactions, and interactions in atomic Bose-Einstein condensates or quantum Fermi gases, describing coherent molecule formation together with s -wave scattering. The simplest two-particle quantum solitons or bound-state solutions of the idealized Hamiltonian, without a momentum cutoff, are obtained exactly. They have a pointlike structure in two and three dimensions—even though the corresponding classical theory is nonsingular. We show that the solutions can be regularized with a momentum cutoff. The parametric quantum solitons have much more realistic length scales and binding energies than $\chi^{(3)}$ quantum solitons, and the resulting effects could potentially be experimentally tested in highly nonlinear optical parametric media or interacting matter-wave systems. N -particle quantum solitons and the ground state energy are analyzed using a variational approach. Applications to atomic/molecular Bose-Einstein condensates (BEC's) are given, where we predict the possibility of forming coupled BEC solitons in three space dimensions, and analyze “superchemistry” dynamics.

PACS number(s): 42.65.Tg, 03.65.Ge, 03.75.Fi, 11.10.St

I. INTRODUCTION

Quantum solitons [1] or bound states of interacting fields are generalizations of nonlinear solitonic solutions of classical wave theory to include quantum fields. Exactly solvable cases include many-body bound states of bosons interacting via a δ -function potential in one space dimension. This model (often called the nonlinear Schrödinger model) was solved by Lieb, Liniger, McGuire, and Yang [2]. Recently it was predicted that this solvable model could lead to experimentally observable quantum effects including quantum squeezing in optical fiber solitons [3,4]. This prediction has now been verified experimentally [5].

Other examples of exactly soluble models are generally restricted either to one space dimension, or to physically inaccessible systems like the quantum Davey-Stewartson model [6]. An exception is Laughlin's highly innovative theory of a two-dimensional electron gas in an external magnetic field [7], which was able to explain the fractional quantum Hall effect [8]. Similar techniques have recently been proposed for treating interacting Bose gases in higher dimensions, in the limit of very weak couplings, leading to an elementary theory of a quantum vortex [9]. Experimental success in Bose-Einstein condensation of atomic gases [10] makes it possible that quantum soliton behavior could become observable in ultralow-temperature nonlinear atom optics, as well as with photons.

In a recent paper [11], we showed that it is possible to obtain an exact solution in one, two, and three space dimensions, in a nonlinear quantum field theory that includes the most fundamental property that distinguishes quantum mechanics from quantum field theory—that is, the ability to create and destroy particles. The simplest cubic interaction involving two boson fields—the parametric interaction of the form $\Psi_1^2\Psi_2^\dagger$ —was analyzed for bound states in higher dimensions, resulting in soluble cases with unusual and unex-

pected properties. This degenerate parametric theory—with similarities to the Friedberg-Lee [12] model of high- T_C superconductivity—has bound states in one space dimension [13,14], but is unstable (like the nonlinear Schrödinger model with an attractive δ -function potential) in higher dimensions. Unlike the nonlinear Schrödinger model, the instability does not occur at the classical level. Indeed, classical parametric solitons in higher dimensions are both theoretically predicted [15–17] and observed to exist [18]. With the inclusion of an additional (repulsive) quartic interaction term in the Hamiltonian, a rigorous lower bound to the energy was proved to exist, and we demonstrated the existence of exact two-particle bound states in higher dimensions [11,19]. These new types of quantum solitons have a finite binding energy, but the corresponding two-particle wave function has a zero radius; the pointlike structure of these bound states can be termed a “quantum singularity.” With a momentum cutoff imposed on the couplings, the bound states develop a finite radius.

In the present paper, we extend these earlier results to include the nondegenerate case of parametric interaction [20] of three distinct fields with either Bose or Fermi statistics (rather than two bosonic fields). The results demonstrate the existence of exact two-particle nondegenerate eigenstates in higher dimensions, having a pointlike structure in space, with a finite energy when there is no momentum cutoff. However, typical physical systems that can be experimentally identified as having the requisite three-wave bosonic interactions usually have momentum cutoffs. These cutoffs, of course, provide a spatial extent to the bound states. We therefore provide solutions that include cutoff effects as well. Estimates of typical binding energies and soliton characteristic radii are given for photonic interactions in highly nonlinear optical materials. They appear to be of more realistic magnitudes for possible experiments, as compared to earlier known quantum solitons based on cubic nonlinearities (see, e.g., [2,21], and [11,14] for comparison).

In addition, we discuss the application of the basic model to coherently coupled atomic/molecular Bose-Einstein condensates (BEC's). This provides the possibility of extending our earlier results [22] on “superchemistry” in degenerate parametric interactions to a larger variety of interacting quantum gases, i.e., to three-species (two atomic and one molecular) BEC systems. We present here a mean-field theory analysis which predicts, at large particle number, a transition to a classical soliton domain, where stable three-dimensional BEC solitons can form in certain parameter ranges.

II. MODEL

We start by considering the following quantum effective Hamiltonian:

$$\hat{H} = \hat{H}_0 + \hat{H}_{int}, \quad (1)$$

where

$$\hat{H}_0 = \hbar \int d^D \mathbf{x} \left(\sum_{i=1}^3 \frac{\hbar}{2m_i} |\nabla \Psi_i(\mathbf{x})|^2 + \Delta \omega \Psi_3^\dagger(\mathbf{x}) \Psi_3(\mathbf{x}) \right), \quad (2)$$

and $\hat{H}_{int} = \hat{H}_{int}^{(\chi)} + \hat{H}_{int}^{(\kappa)}$, with

$$\begin{aligned} \hat{H}_{int}^{(\chi)} = & \hbar \int \int \int d^D \mathbf{x} d^D \mathbf{y} d^D \mathbf{z} \chi_D(\mathbf{x}, \mathbf{y}, \mathbf{z}) \\ & \times [\Psi_1(\mathbf{x}) \Psi_2(\mathbf{y}) \Psi_3^\dagger(\mathbf{z}) + \text{H.c.}], \end{aligned} \quad (3)$$

$$\begin{aligned} \hat{H}_{int}^{(\kappa)} = & \frac{\hbar}{2} \sum_{i,j=1}^3 \int \int \int \int d^D \mathbf{x} d^D \mathbf{y} d^D \mathbf{x}' d^D \mathbf{y}' \kappa_D^{(ij)}(\mathbf{x}, \mathbf{y}, \mathbf{x}', \mathbf{y}') \\ & \times \Psi_i^\dagger(\mathbf{x}) \Psi_j^\dagger(\mathbf{y}) \Psi_i(\mathbf{x}') \Psi_j(\mathbf{y}'). \end{aligned} \quad (4)$$

Here Ψ_1 , Ψ_2 , and Ψ_3 are three Bose fields with commutation relations $[\Psi_i(\mathbf{x}), \Psi_j^\dagger(\mathbf{x}')] = \delta_{ij} \delta(\mathbf{x} - \mathbf{x}')$. In addition, m_1 , m_2 , and m_3 are the corresponding effective masses and $\Delta \omega$ is the phase mismatch or the bare formation energy of the field Ψ_3 . Nonlinear interactions are included via the parametric interaction potential χ_D describing a particle number nonconserving process, in which a pair of Ψ_1 and Ψ_2 quanta is destroyed and a Ψ_3 quantum is created, while $\kappa_D^{(ij)}$ is the particle number conserving potential describing quartic self- and cross-interactions between the fields, in D ($D=1,2,3$) space dimensions.

In the case of optical interactions the couplings are due to quadratic and cubic polarizabilities of the nonlinear medium, giving rise to the parametric process of frequency conversion (sum-frequency generation), together with self- and cross-phase modulation processes. The above effective Hamiltonian can also be applied to describe nonlinear interactions of matter-wave fields, such as in coupled atomic (Ψ_1 and Ψ_2 fields) and molecular (Ψ_3 field) Bose condensates. In this case, the parametric coupling χ_D would refer to the rate of coherent process of atomic dimerization, where pairs of at-

oms (of masses m_1 and m_2) convert into diatomic molecules (of mass $m_3 = m_1 + m_2$), while the quartic couplings $\kappa_D^{(ij)}$ would refer to the strength of intra- and interspecies two-body collisions.

In the case of degenerate couplings ($\Psi_1 = \Psi_2$), the coherent process of dimerization in atomic/molecular BEC interactions and the possibility of formation of coupled atomic-molecular solitons has been studied in [19,22,23]. Pure quartic interactions in two-species Bose condensates have been analyzed in [24], while the interplay between parametric and (attractive) quartic interactions in optical soliton propagation, at the classical level, has been studied in [25].

An important feature encountered in the treatment of the present nondegenerate parametric interaction is that, although we have specified Bose statistics for all three interacting fields Ψ_i , some of the results obtained here will also be valid if fermionic fields are involved and the corresponding commutators are replaced by anticommutators. An example of such systems is the case where Ψ_1 and Ψ_2 are fermionic, as in the “ s -channel” model of high- T_C superconductivity by Friedberg and Lee [12]. Similarly, the case where Ψ_2 and Ψ_3 are fermionic, as in the Lee–Van Hove model of nuclear interactions [26], is also treatable.

To simplify the theory we consider in Sec. III the approximation in which we assume short range interactions and, taking into account translational invariance considerations, replace the interaction potentials by δ function pseudopotentials. In this case, the interacting part of the Hamiltonian is

$$\begin{aligned} \hat{H}_{int} = & \hbar \int d^D \mathbf{x} \left(\chi_D [\Psi_1(\mathbf{x}) \Psi_2(\mathbf{x}) \Psi_3^\dagger(\mathbf{x}) \right. \\ & + \Psi_1^\dagger(\mathbf{x}) \Psi_2^\dagger(\mathbf{x}) \Psi_3(\mathbf{x})] \\ & + \sum_{i,j=1}^3 \frac{1}{2} \kappa_D^{(ij)} \Psi_i^\dagger(\mathbf{x}) \Psi_j^\dagger(\mathbf{x}) \Psi_i(\mathbf{x}) \Psi_j(\mathbf{x}) \left. \right). \end{aligned} \quad (5)$$

This is a very idealized model. We note that such models in quantum field theory are usually treated in the context of renormalized perturbation theory, with the understanding that the coupling constants are a function of an implicit momentum cutoff. However, we shall demonstrate a rather unexpected and remarkable result, which is that the above idealized Hamiltonian has an exact ground state with a finite binding energy—even without a cutoff or renormalization procedure. We emphasize that provided $\kappa_D^{(ij)} > 0$ there are no energy divergences or collapsing behavior in this idealized cubic-quartic model, unlike the case of a Bose gas with purely quartic attractive δ -function interactions. On the other hand, for a Bose gas with purely quartic repulsive δ -function interactions the exact eigenvalues in more than one dimension are the same as those for free particles, i.e., the δ -function pseudopotential produces no scattering and the ground state energy is the same as for a noninteracting Bose gas [27]. Instead, the idealized model we consider gives a nontrivial bound state that has a finite binding energy, but involves a pointlike (zero-radius) structure in more than one space dimension. While physical models typically do have a

momentum cutoff, the exactly soluble model without cutoff is indicative of behavior with a cutoff, and provides some useful insight.

A more sophisticated pseudopotential approach would be to employ the regularized method used by Huang, Yang, and Lee [28]. However, for simplicity we choose to start with a simple Dirac δ -function interaction which has the advantage of giving a Hermitian Hamiltonian. More careful treatment of the δ -function interaction would be to incorporate a momentum cutoff imposed on the nonlinear couplings. This is further treated in Sec. IV, where we obtain a regularized bound state with a finite spatial extent in one, two, and three dimensions.

III. CUTOFF INDEPENDENT RESULTS

To construct the general candidate for the eigenstate to the Hamiltonian given by Eqs. (1), (2), and (5), we note that the parametric interaction transforms pairs of $\hat{\Psi}_1$ and $\hat{\Psi}_2$ quanta into single $\hat{\Psi}_3$ quanta, and vice versa. That is, the Hamiltonian does not conserve the corresponding particle numbers. However, it does conserve a generalized particle number, or Manley-Rowe invariant, equal to

$$\hat{N} = \hat{N}_1 + \hat{N}_2 + 2\hat{N}_3 = \int d^D \mathbf{x} (|\hat{\Psi}_1|^2 + |\hat{\Psi}_2|^2 + 2|\hat{\Psi}_3|^2). \quad (6)$$

In addition, the Hamiltonian is translationally invariant, and thus conserves the total momentum given by

$$\hat{\mathbf{P}} = \hbar \hat{\mathbf{K}} = -\frac{i\hbar}{2} \int d^D \mathbf{x} \sum_{i=1}^3 [\hat{\Psi}_i^\dagger (\nabla \hat{\Psi}_i) - (\nabla \hat{\Psi}_i^\dagger) \hat{\Psi}_i]. \quad (7)$$

We therefore search for states $|\varphi_{\mathbf{K}}^{(N)}\rangle$ that are eigenstates of \hat{H} , \hat{N} , and $\hat{\mathbf{K}}$, with energy eigenvalues $E_{\mathbf{K}}^{(N)}$.

A. Two-particle eigenvalue equation

We consider first the two-particle ($N=2$) eigenstate which must have the form of a superposition state:

$$|\varphi_{\mathbf{K}}^{(2)}\rangle = \left(\int d^D \mathbf{x} P(\mathbf{x}) \hat{\Psi}_3^\dagger(\mathbf{x}) + \int \int d^D \mathbf{x} d^D \mathbf{y} Q(\mathbf{x}, \mathbf{y}) \hat{\Psi}_1^\dagger(\mathbf{x}) \hat{\Psi}_2^\dagger(\mathbf{y}) \right) |0\rangle, \quad (8)$$

where P and Q are one- and two-particle wave functions, respectively.

We note that the quartic terms in the interaction Hamiltonian (5) other than the cross-interaction term between the $\hat{\Psi}_1$ and $\hat{\Psi}_2$ fields have no effect on the two-particle eigenstate. For this reason, we will use a simplified notation

$$\kappa_D \equiv (\kappa_D^{(12)} + \kappa_D^{(21)})/2 = \kappa_D^{(12)} \quad (9)$$

for the cross-coupling between the fields $\hat{\Psi}_1$ and $\hat{\Psi}_2$.

Operating on $|\varphi_{\mathbf{K}}^{(2)}\rangle$, Eq. (8), with the Hamiltonian (1), (2), and (5) gives that the two-particle eigenvalue problem $\hat{H}|\varphi_{\mathbf{K}}^{(2)}\rangle = E_{\mathbf{K}}^{(2)}|\varphi_{\mathbf{K}}^{(2)}\rangle$ is equivalent to the following set of equations:

$$\frac{\hbar^2}{2m_3} \nabla^2 P(\mathbf{x}) + (E_{\mathbf{K}}^{(2)} - \hbar \Delta \omega) P(\mathbf{x}) = \hbar \chi_D Q(\mathbf{x}, \mathbf{x}), \quad (10)$$

$$\begin{aligned} & \left(\frac{\hbar^2}{2m_1} \nabla_{\mathbf{x}}^2 + \frac{\hbar^2}{2m_2} \nabla_{\mathbf{y}}^2 \right) Q(\mathbf{x}, \mathbf{y}) + E_{\mathbf{K}}^{(2)} Q(\mathbf{x}, \mathbf{y}) \\ & = \hbar \left[\chi_D P \left(\frac{m_1 \mathbf{x} + m_2 \mathbf{y}}{m_1 + m_2} \right) + \kappa_D Q(\mathbf{x}, \mathbf{y}) \right] \delta(\mathbf{x} - \mathbf{y}), \end{aligned} \quad (11)$$

where $E_{\mathbf{K}}^{(2)}$ is the corresponding energy eigenvalue.

To solve these equations we introduce the relative and center-of-mass coordinates according to $\mathbf{r} = \mathbf{x} - \mathbf{y}$ and $\mathbf{R} = (m_1 \mathbf{x} + m_2 \mathbf{y})/(m_1 + m_2)$. With these coordinates we have

$$\frac{\hbar^2}{2m_1} \nabla_{\mathbf{x}}^2 + \frac{\hbar^2}{2m_2} \nabla_{\mathbf{y}}^2 = \frac{\hbar^2}{2M} \nabla_{\mathbf{R}}^2 + \frac{\hbar^2}{2\mu} \nabla_{\mathbf{r}}^2, \quad (12)$$

where we have introduced a reduced mass

$$\mu = \frac{m_1 m_2}{m_1 + m_2}, \quad (13)$$

and defined $M \equiv m_1 + m_2$. Assuming translational invariance we can seek for $P(\mathbf{x})$ in the form of $P(\mathbf{x}) = P_0 \exp(i\mathbf{K} \cdot \mathbf{x})$, where \mathbf{K} is the total momentum. As a consequence, $Q(\mathbf{x}, \mathbf{x})$ will be proportional to $P(\mathbf{x})$, and therefore we may look for the general expression for $Q(\mathbf{x}, \mathbf{y})$ in a separable form: $Q(\mathbf{x}, \mathbf{y}) = g(\mathbf{r}) P(\mathbf{R})$. Substituting this into Eqs. (10) and (11), and dividing the energy into center-of-mass and relative components $E_{\mathbf{K}}^{(2)} = E_c + E_r$, we then solve the equation for $P(\mathbf{R})$, yielding at $P(\mathbf{R}) = P_0 \exp(i\mathbf{K} \cdot \mathbf{R})$, with $K^2 = |\mathbf{K}|^2 = 2ME_c/\hbar^2$, and as a result

$$E_{\mathbf{K}}^{(2)} = \hbar^2 K^2 / (2m_3) + \hbar \Delta \omega + \hbar \chi_D g(0). \quad (14)$$

The remaining equation for the $g(\mathbf{r})$ function is rewritten as

$$\nabla^2 g(\mathbf{r}) - r_0^{-2} g(\mathbf{r}) = \frac{2\mu}{\hbar} [\chi_D + \kappa_D g(0)] \delta(\mathbf{r}), \quad (15)$$

where we have defined a length scale r_0 , according to

$$r_0^{-2} = -\frac{2\mu E_r}{\hbar^2} = \frac{\mu K^2}{M} - \frac{2\mu E_{\mathbf{K}}^{(2)}}{\hbar^2}. \quad (16)$$

Together with Eq. (14), this implies that the energy eigenvalue is given by

$$E_{\mathbf{K}}^{(2)} = \frac{\hbar^2 K^2}{2M} - \frac{\hbar^2}{2\mu r_0^2}, \quad (17)$$

where r_0 is to be found by solving the following eigenvalue equation:

$$r_0^{-2} = \frac{2\mu}{\hbar} [\Delta - \chi_D g(0)]. \quad (18)$$

Here r_0 must be real and positive for a localized bound state or quantum soliton solution. The quantity

$$E_b^{(2)} \equiv \frac{\hbar^2}{2\mu r_0^2} = \hbar \Delta - \hbar \chi_D g(0) \quad (19)$$

can be interpreted as the binding energy of the two-particle quantum soliton with the momentum \mathbf{K} , and we have defined

$$\Delta \equiv \frac{\hbar}{2} \left(\frac{K^2}{M} - \frac{K^2}{m_3} \right) - \Delta \omega. \quad (20)$$

Equations (17) and (18) are equivalent to formulating the eigenvalue problem directly in terms of Eq. (14), where $g(0)$ is to be found by solving the following equation:

$$\nabla^2 g(\mathbf{r}) - \frac{2\mu}{\hbar} [\Delta - \chi_D g(0)] g(\mathbf{r}) = \frac{2\mu}{\hbar} [\chi_D + \kappa_D g(0)] \delta(\mathbf{r}). \quad (21)$$

Thus, the two-particle (or diboson) eigenstate candidate (8) that is a simultaneous eigenstate of the momentum operator takes the following form:

$$|\varphi_{\mathbf{K}}^{(2)}\rangle = \left[\int d^D \mathbf{x} e^{i\mathbf{K} \cdot \mathbf{x}} \hat{\Psi}_3^\dagger(\mathbf{x}) + \int \int d^D \mathbf{r} d^D \mathbf{R} e^{i\mathbf{K} \cdot \mathbf{R}} g(\mathbf{r}) \right. \\ \left. \times \hat{\Psi}_1^\dagger\left(\mathbf{R} + \frac{m_2 \mathbf{r}}{M}\right) \hat{\Psi}_2^\dagger\left(\mathbf{R} - \frac{m_1 \mathbf{r}}{M}\right) \right] |0\rangle. \quad (22)$$

B. Energy lower bound for two-particle case

The stability of our Hamiltonian in the two-particle sector can be proved by finding a lower bound E_l to the Hamiltonian energy, $E_{\mathbf{K}}^{(2)} = \langle \varphi_{\mathbf{K}}^{(2)} | \hat{H} | \varphi_{\mathbf{K}}^{(2)} \rangle / \langle \varphi_{\mathbf{K}}^{(2)} | \varphi_{\mathbf{K}}^{(2)} \rangle$, so that $E_{\mathbf{K}}^{(2)} \geq E_l$. Applying the Hamiltonian to $|\varphi_{\mathbf{K}}^{(2)}\rangle$, and using the symmetry property of the two-particle correlation function $g(\mathbf{x}) = g(-\mathbf{x})$, one can find that

$$E_{\mathbf{K}}^{(2)} = \left(1 + \int d^D \mathbf{r} g^2(\mathbf{r}) \right)^{-1} \left(\frac{\hbar^2}{2\mu} \int d^D \mathbf{r} |\nabla g(\mathbf{r})|^2 \right. \\ \left. + \frac{\hbar^2 K^2}{2M} \int d^D \mathbf{r} g^2(\mathbf{r}) + \frac{\hbar^2 K^2}{2m_3} + \hbar \Delta \omega + 2\hbar \chi_D g(0) \right. \\ \left. + \hbar \kappa_D g^2(0) \right). \quad (23)$$

Omitting the first nonnegative term in the square brackets, we arrive at a lower energy that is rigorously bounded from below if $\kappa_D > 0$, according to

$$E_{\mathbf{K}}^{(2)} \geq \frac{\hbar^2 K^2}{2M} + \frac{\hbar \kappa_D g^2(0) + 2\hbar \chi_D g(0) - \hbar \Delta}{1 + \int d^D \mathbf{r} g^2(\mathbf{r})} \\ \geq \frac{\hbar^2 K^2}{2M} - \frac{\hbar (\chi_D^2 + \Delta \kappa_D)}{\kappa_D \left[1 + \int d^D \mathbf{r} g^2(\mathbf{r}) \right]}, \quad (24)$$

where Δ is defined in Eq. (20).

If $(\chi_D)^2 + \Delta \kappa_D \leq 0$, then the lower bound E_l is given by $E_l = \hbar^2 K^2 / (2M) = E_c$. This has a simple interpretation as providing the center-of-mass energy, so that $E_{\mathbf{K}}^{(2)} \geq E_c$ (or $E_r = E_{\mathbf{K}}^{(2)} - E_c \geq 0$) and no bound states, with $E_r = E_{\mathbf{K}}^{(2)} - E_c < 0$, are possible in this case. If, however,

$$(\chi_D)^2 + \Delta \kappa_D > 0, \quad (25)$$

which is the case that we focus on in this paper, then we have

$$E_{\mathbf{K}}^{(2)} \geq \frac{\hbar^2 K^2}{2M} - \hbar \Delta - \frac{\hbar (\chi_D)^2}{\kappa_D} \\ = \frac{\hbar^2 K^2}{2m_3} + \hbar \Delta \omega - \frac{\hbar (\chi_D)^2}{\kappa_D} \equiv E_l. \quad (26)$$

This implies that $E_r = E_{\mathbf{K}}^{(2)} - E_c \geq \hbar \Delta \omega - \hbar (\chi_D)^2 / \kappa_D$, and bound states may become available.

C. Exact diboson solutions

Equations (15) and (18) can easily be analyzed using the Fourier transform method. In this approach we seek a solution to Eq. (15) in the form

$$g(r) = \int d^D \mathbf{k} G(\mathbf{k}) \exp(i\mathbf{k} \cdot \mathbf{r}) / (2\pi)^D,$$

where $r = |\mathbf{r}|$. Expanding the δ function into a Fourier integral, we then obtain the Fourier transform equivalent to Eq. (15):

$$(k^2 + r_0^{-2}) G(\mathbf{k}) = -q, \quad (27)$$

where $k = |\mathbf{k}|$, and we have defined

$$q \equiv 2\mu [\chi_D + \kappa_D g(0)] / \hbar. \quad (28)$$

Solving Eq. (27) for $G(\mathbf{k})$ and substituting it into the expression for $g(r)$ we find

$$g(r) = -\frac{q}{(2\pi)^D} \int d^D \mathbf{k} \frac{\exp(i\mathbf{k} \cdot \mathbf{r})}{k^2 + 1/r_0^2}. \quad (29)$$

1. One-dimensional case ($D=1$)

In the one-dimensional case ($D=1$) the integration gives

$$g(r) = -\frac{q}{2\pi} \int_{-\infty}^{+\infty} dk \frac{\exp(ikr)}{k^2 + 1/r_0^2} = -\frac{qr_0}{2} \exp(-|r|/r_0). \quad (30)$$

Using this result at $r=0$ and the definition of q , we solve for $g(0)$ and find that $g(0) = -\chi_1[\kappa_1 + \hbar/(\mu r_0)]^{-1}$. Correspondingly, the eigenvalue equation (18) for r_0 is now rewritten as a cubic:

$$\frac{2\mu^2}{\hbar^2}[(\chi_1)^2 + \Delta\kappa_1]r_0^3 + \frac{2\mu\Delta}{\hbar}r_0^2 - \frac{\mu\kappa_1}{\hbar}r_0 - 1 = 0, \quad (31)$$

where r_0 must be real and positive for a localized bound state.

The analysis of this equation shows that if $\kappa_1 > 0$ and $(\chi_1)^2 + \Delta\kappa_1 > 0$ —that is, under the same conditions that we assumed while proving the lower bound, Eq. (26)—then there always exists one positive solution for r_0 . This proves the existence of a one-dimensional two-particle quantum soliton, with a characteristic radius r_0 and a binding energy of $E_b^{(2)} = \hbar^2/(2\mu r_0^2)$. In the absence of the quartic term ($\kappa_1 = 0$) and with perfect phase matching $\Delta\omega = 0$ and $m_3 = M$ (so that $\Delta = 0$), the equation for r_0 is solved analytically. This gives the following explicit results for the soliton binding energy and the radius:

$$E_b^{(2)} = (\hbar^2\mu/2)^{1/3}(\chi_1)^{4/3}, \quad (32)$$

$$r_0 = (\hbar^2/2\chi_1^2\mu^2)^{1/3}. \quad (33)$$

2. Higher-dimensional case ($D=2,3$)

The two- and three-dimensional results are qualitatively different. In these cases we evaluate the integrals for $g(0)$, from Eq. (29), in polar (for $D=2$) and spherical (for $D=3$) coordinates. Using the definition of q , we then solve for $g(0)$ and obtain $g(0) = -\chi_D[\kappa_D + \hbar r_0^{D-2}/(2\mu f_D)]^{-1}$, where we have defined the dimensionless integral

$$f_D = \frac{1}{2\pi^{D-1}} \int_0^\infty dx \frac{x^{D-1}}{1+x^2} \quad (D=2,3). \quad (34)$$

This integral diverges for $D=2,3$. (A strict treatment of this divergence, as a mathematical limit, is given in Sec. IV, where it is attributed to $k_m \rightarrow \infty$, with k_m being the upper limit in the integral.) Therefore we find that $g(0)$ and hence the energy eigenvalue $E_{\mathbf{K}}^{(2)}$ from Eq. (14) are given by

$$g(0) = -\chi_D/\kappa_D, \quad (35)$$

$$E_{\mathbf{K}}^{(2)} = \frac{\hbar^2 K^2}{2m_3} + \hbar\Delta\omega - \frac{\hbar(\chi_D)^2}{\kappa_D} \quad (D=2,3). \quad (36)$$

With the above result for $g(0)$ it also follows that $q=0$, and since the integral in Eq. (29) converges for $r \neq 0$, we obtain that $g(r)=0$ if $r \neq 0$. This means that the exact bound-state solution in two and three dimensions have a pointlike (zero-radius) structure, which is in the relative positions of the $\hat{\Psi}_1$ and $\hat{\Psi}_2$ quanta.

Thus, the results of this section show that our model Hamiltonian provides quantum solitons or two-particle (diboson) eigenstates in one and more space dimensions. An important difference between the one-dimensional and mul-

tidimensional solutions is in their structure and dependence on the additional quartic interaction. In one dimension the bound state has finite characteristic size and is available even without a quartic term in the Hamiltonian. In two and three dimensions, the bound states involve a pointlike structure, yet the corresponding binding energy is finite, if $\kappa_D > 0$. If, however, $\kappa_D = 0$ we obtain an energy collapse: $E_{\mathbf{K}}^{(2)} \rightarrow -\infty$. Thus, while the additional quartic interaction prevents an energy collapse and makes multidimensional quantum solitons possible, these solitons involve a zero-radius relative localization of the $\hat{\Psi}_1$ and $\hat{\Psi}_2$ quanta.

The diboson solutions can be regarded as a type of dressing of the $\hat{\Psi}_3$ quanta, which have a lower energy due to the creation of virtual pairs of $\hat{\Psi}_1$ and $\hat{\Psi}_2$ quanta. We also note that in a renormalized theory in which χ_D and κ_D are regarded as functions of a momentum cutoff k_m , the above result implies that $(\chi_D)^2/\kappa_D$ must approach a constant value at large k_m , in order that the observed binding energy should be cutoff independent.

D. Energy lower bound for N -particle case

The zero-radius form of the two-particle bound states in two and three space dimensions simplifies the treatment of the general case of N -particle bound states, so that one can find an *exact* ground state solution to this quantum many-body system. To show this first we prove a lower bound to the Hamiltonian energy in the N -particle sector. To do so we neglect the non-negative kinetic energy term $\{\hat{H}_{kin} = \int d^D \mathbf{x} [\sum_{i=1}^3 (\hbar^2/2m_i) |\nabla \hat{\Psi}_i|^2]\}$ in the Hamiltonian and consider a reduced Hamiltonian $\hat{H}_R = \hat{H} - \hat{H}_{kin}$, such that $\hat{H} \geq \hat{H}_R$. Assuming that $\kappa_D > 0$, one can show that

$$\begin{aligned} \hat{H}_R \geq & \hbar[\Delta\omega - (\chi_D)^2/\kappa_D] \int d^D \mathbf{x} \hat{\Psi}_3^\dagger \hat{\Psi}_3 \\ & + \hbar \int d^D \mathbf{x} \left(\sum_{i=1}^3 \frac{1}{2} \kappa_D^{(ii)} \hat{\Psi}_i^\dagger \hat{\Psi}_i^2 + \kappa_D^{(13)} \hat{\Psi}_1^\dagger \hat{\Psi}_1 \hat{\Psi}_3^\dagger \hat{\Psi}_3 \right. \\ & \left. + \kappa_D^{(23)} \hat{\Psi}_2^\dagger \hat{\Psi}_2 \hat{\Psi}_3^\dagger \hat{\Psi}_3 \right), \end{aligned} \quad (37)$$

which is simply seen by substituting the expression for \hat{H}_R and rewriting this inequality in the form

$$\frac{1}{\kappa_D} \int d^D \mathbf{x} |\kappa_D \hat{\Psi}_1^\dagger \hat{\Psi}_2^\dagger + \chi_D \hat{\Psi}_3|^2 \geq 0. \quad (38)$$

Combining now the inequality $\hat{H} \geq \hat{H}_R$ and Eq. (37), and assuming that all the other quartic couplings are non-negative ($\kappa_D^{(ii)}, \kappa_D^{(13)}, \kappa_D^{(23)} \geq 0$) we arrive at

$$\hat{H} \geq \hbar \left(\Delta\omega - \frac{(\chi_D)^2}{\kappa_D} \right) \int d^D \mathbf{x} \hat{\Psi}_3^\dagger \hat{\Psi}_3, \quad (39)$$

implying that the energy eigenvalue $E_{\mathbf{K}}^{(N)} = \langle \varphi_{\mathbf{K}}^{(N)} | \hat{H} | \varphi_{\mathbf{K}}^{(N)} \rangle / \langle \varphi_{\mathbf{K}}^{(N)} | \varphi_{\mathbf{K}}^{(N)} \rangle$ satisfies the following inequality:

$$E_{\mathbf{K}}^{(N)} \geq \hbar \left(\Delta \omega - \frac{(\chi_D)^2}{\kappa_D} \right) \bar{N}_3, \quad (40)$$

where $\bar{N}_i \equiv \langle \varphi_{\mathbf{K}}^{(N)} | \hat{N}_i | \varphi_{\mathbf{K}}^{(N)} \rangle / \langle \varphi_{\mathbf{K}}^{(N)} | \varphi_{\mathbf{K}}^{(N)} \rangle$.

Due to the conservation of the generalized particle number $\hat{N} = \hat{N}_1 + \hat{N}_2 + 2\hat{N}_3$, we have $\bar{N}_3 \leq [N/2]$, where $[N/2]$ is the integer part of $N/2$. Therefore, if

$$\Delta \omega - \frac{(\chi_D)^2}{\kappa_D} < 0, \quad (41)$$

we obtain, from Eq. (40),

$$E_{\mathbf{K}}^{(N)} \geq [N/2] \left(\hbar \Delta \omega - \frac{\hbar (\chi_D)^2}{\kappa_D} \right) \equiv E_l^{(N)}. \quad (42)$$

This proves the lower bound $E_l^{(N)}$ to the Hamiltonian energy, which we note is valid in one, two, and three dimensions.

In two and three dimensions the above inequality can be further simplified. Since the expression $\hbar \Delta \omega - \hbar (\chi_D)^2 / \kappa_D$ represents [see Eq. (36)] the exact two-particle energy eigenvalue with zero momentum, $E_0^{(2)}$, we can rewrite Eq. (42) as

$$E_{\mathbf{K}}^{(N)} \geq E_l^{(N)} = [N/2] E_0^{(2)} \quad (D=2,3). \quad (43)$$

E. Exact N -particle ground state ($D=2,3$)

We can now use the lower bound to obtain the zero-momentum energy eigenvalue $E_0^{(N)}$ for any even particle number N in more than one space dimensions, and without the $\hat{\Psi}_3$ self-interaction term. In order to understand the physical meaning of these results, we introduce a finite quantization volume V in this section, to give a finite density. The technique to find $E_0^{(N)}$ is extremely simple. We will demonstrate that there is an upper bound to the Hamiltonian ground state energy, that coincides with the lower bound given above, in either the case that $\kappa_D^{(33)} = 0$ (no $\hat{\Psi}_3$ self-interaction) or the case that $V \rightarrow \infty$ (infinite volume). The result in the infinite volume limit is expected, as it corresponds to an infinitely dilute gas of the diboson ($|\varphi_0^{(2)}\rangle$) bound states. However, the same result also holds at finite volume provided there is no $\hat{\Psi}_3$ self-interaction term.

In order to estimate the ground state energy $E_0^{(N)}$, in two and three dimensions, we employ a trial wave function that gives an upper bound $\tilde{E}_0^{(N)}$ to the energy $E_0^{(N)}$. We use an ansatz that represents $N/2$ (where we assume N is even) independent two-particle quantum solitons or dibosons with $\mathbf{K} = \mathbf{0}$:

$$|\tilde{\varphi}_0^{(N)}\rangle = \left[\int d^D \mathbf{x} \hat{\Psi}_3^\dagger(\mathbf{x}) + \int \int d^D \mathbf{r} d^D \mathbf{R} g(\mathbf{r}) \times \hat{\Psi}_1^\dagger\left(\mathbf{R} + \frac{m_2 \mathbf{r}}{M}\right) \hat{\Psi}_2^\dagger\left(\mathbf{R} - \frac{m_1 \mathbf{r}}{M}\right) \right]^{N/2} |0\rangle. \quad (44)$$

Here $g(\mathbf{r})$ is the zero-radius two-particle correlation function found earlier, having the property that $\int d^D \mathbf{r} g^2(\mathbf{r}) = 0$ and $g(0) = -\chi_D / \kappa_D$, in two and three dimensions. Calculating the energy $\tilde{E}_0^{(N)} = \langle \tilde{\varphi}_0^{(N)} | \hat{H} | \tilde{\varphi}_0^{(N)} \rangle / \langle \tilde{\varphi}_0^{(N)} | \tilde{\varphi}_0^{(N)} \rangle$ with the ansatz (44) gives (see Appendix A)

$$\tilde{E}_0^{(N)} = \frac{N}{2} \left(\hbar \Delta \omega - \frac{\hbar (\chi_D)^2}{\kappa_D} \right) + \frac{N}{2} \left(\frac{N}{2} - 1 \right) \frac{\hbar \kappa_D^{(33)}}{V} \quad (D=2,3), \quad (45)$$

where $V = \int d^D \mathbf{x}$ is the integration volume. The self-interaction terms of the fields $\hat{\Psi}_1$ and $\hat{\Psi}_2$ ($\sim \kappa_D^{(11)}$ and $\kappa_D^{(22)}$), as well as the cross-interaction terms between the fields $\hat{\Psi}_{1,2}$ and $\hat{\Psi}_3$ ($\sim \kappa_D^{(13)}$ and $\kappa_D^{(23)}$), do not contribute to the energy $\tilde{E}_0^{(N)}$. The first term in Eq. (45) is simply the energy due to $N/2$ independent noninteracting dibosons, each having the energy $E_0^{(2)}$, Eq. (36). The second term in Eq. (45) is the self-interaction energy of the $\hat{\Psi}_3$ field, which depends explicitly on the interaction volume V and decreases as V is increased.

The above result is easier to understand if we calculate the average number of quanta $\bar{N}_i = \langle \tilde{\varphi}_0^{(N)} | \hat{N}_i | \tilde{\varphi}_0^{(N)} \rangle / \langle \tilde{\varphi}_0^{(N)} | \tilde{\varphi}_0^{(N)} \rangle$ in each field, which gives $\bar{N}_3 = N/2$ and $\bar{N}_{1,2} = 0$. This implies that the $\hat{\Psi}_1$ and $\hat{\Psi}_2$ quanta can only be regarded as virtual, the presence of which is manifested by the finite binding energy of the two-particle bound states. In such a virtual state, the $\hat{\Psi}_1$ and $\hat{\Psi}_2$ quanta can only interact via the parametric χ_D and the quartic cross-coupling κ_D within the individual dibosons. This is a consequence of the zero-radius property of the two-particle correlation function $g(\mathbf{r})$ employed in the ansatz (44).

Using Eq. (36), we can rewrite Eq. (45) as

$$\tilde{E}_0^{(N)} = \frac{N}{2} E_0^{(2)} + \frac{N}{4} \left(\frac{N}{2} - 1 \right) \frac{\hbar \kappa_D^{(33)}}{V} \quad (D=2,3). \quad (46)$$

Comparing this result with the lower bound $E_l^{(N)}$ [Eq. (43)] we see that the energy $\tilde{E}_0^{(N)}$ coincides with $E_l^{(N)}$ if $\kappa_D^{(33)} = 0$. This implies that, in the absence of the quartic self-interaction of the $\hat{\Psi}_3$ field, our result for $\tilde{E}_0^{(N)}$ represents the *exact* ground state energy of this quantum many-body system:

$$E_0^{(N)} = \frac{N}{2} E_0^{(2)} = \frac{N}{2} \left(\hbar \Delta \omega - \frac{\hbar (\chi_D)^2}{\kappa_D} \right) \quad (D=2,3), \quad (47)$$

and that the ansatz (44) can be regarded as the exact N -particle eigenstate in this case. The N -particle ground state energy diverges as $\kappa_D \rightarrow 0$. This is in contrast to the behavior of the corresponding classical theory, which has rigorous lower bound to the Hamiltonian energy [15].

For a nonzero $\kappa_D^{(33)}$ the same result, Eq. (47), for the ground state energy would be valid in an infinitely large

volume, corresponding to largely separated and effectively noninteracting dressed $\hat{\Psi}_3$ quanta at a vanishing density. More generally, for a finite interaction volume or a finite density, the above results imply that the ansatz (44) gives an upper bound to the ground state energy. It is possible that the true ground state energy is simply equal to the lower bound $E_l = [N/2]E_0^{(2)}$ in this case as well, in analogy with the treatment of a simple single-component Bose gas with a repulsive δ -function interaction [27], which reproduces the results of the noninteracting theory.

IV. CUTOFF DEPENDENT AND MEAN-FIELD THEORY RESULTS

The zero-radius behavior of the quantum solitons in two and three dimensions represents a rather unusual situation, since the classical counterpart of the bosonic theory has well-behaved, stable, multidimensional soliton solutions [15]. This leads to a paradox of how such a quantum field theory relates to real physical processes. To resolve this paradox, we note that physical applications usually involve some type of momentum cutoff. In systems with dimension $D > 1$ it is known that an effective Hamiltonian of the type we consider here should be renormalized, with a coupling constant that is cutoff dependent, in order to compare the coupling parameters with observable values. Since the exact form of the interaction potentials is not well known, we simply employ a finite bound on the relative momentum.

In the case of nonlinear optical parametric interactions, the cutoff originates from the fact that parametric couplings are usually restricted to a finite range of relative momenta of the interacting fields. To estimate the cutoff in this case, we note that the origins of the theory involve rotating-wave and paraxial approximations, and the neglect of higher-order dispersion [3,29]. Therefore, in higher dimensions we should include nonparaxial diffraction if the characteristic radius of solutions becomes less than the field carrier wavelengths. To represent this we can introduce a cutoff at k_m in the relative momenta \mathbf{k} of the fields $\hat{\Psi}_1$ and $\hat{\Psi}_2$. Since the paraxial approximation is valid only for $k_\perp \ll 2\pi/\lambda_1$, where λ_1 is assumed to be the longest carrier wavelength, then a momentum cutoff of at most $k_m \sim 2\pi/\lambda_1$ should be imposed on the nonlinear couplings. In the case of atomic BEC interactions [30], the cutoff is usually introduced at the level of inverse s -wave scattering length, and a similar cutoff occurs in cases where fermionic fields are involved [12,26].

A. Hamiltonian with momentum cutoff

To implement a cutoff in the interaction part of our Hamiltonian we first consider the parametric interaction term which is of the form of Eq. (3). Assuming translational invariance we note that $\chi_D(\mathbf{x}, \mathbf{y}, \mathbf{z})$ can only depend on the relative coordinates, which we choose according to $\mathbf{x} - \mathbf{y} \equiv \mathbf{r}$ and $\mathbf{z} - \mathbf{R} \equiv \boldsymbol{\xi}$, where $\mathbf{R} = (m_1\mathbf{x} + m_2\mathbf{y})/(m_1 + m_2)$ is the center-of-mass coordinate for the $\hat{\Psi}_1$ and $\hat{\Psi}_2$ fields. That is, $\hat{H}_{int}^{(\chi)}$ can be written as

$$\begin{aligned} \hat{H}_{int}^{(\chi)} = & \hbar \int \int \int d^D \mathbf{r} d^D \mathbf{R} d^D \mathbf{z} \chi_D(\mathbf{r}, \boldsymbol{\xi}) \\ & \times \left[\hat{\Psi}_1^\dagger \left(\mathbf{R} + \frac{m_2 \mathbf{r}}{m_1 + m_2} \right) \hat{\Psi}_2^\dagger \left(\mathbf{R} - \frac{m_1 \mathbf{r}}{m_1 + m_2} \right) \right. \\ & \left. \times \hat{\Psi}_3(\mathbf{R} + \boldsymbol{\xi}) + \text{H.c.} \right], \end{aligned} \quad (48)$$

where we use the same notation χ_D for the translationally invariant coupling potential.

In Fourier space, where

$$\hat{\Psi}_i(\mathbf{x}) = \int d^D \mathbf{k} \hat{a}_i(\mathbf{k}) \exp(i\mathbf{k} \cdot \mathbf{x}) / (2\pi)^{D/2}$$

and the commutation relations for the operators $\hat{a}_i(\mathbf{k})$ and $\hat{a}_i^\dagger(\mathbf{k})$ are $[\hat{a}_i(\mathbf{k}), \hat{a}_j^\dagger(\mathbf{k}')] = \delta_{ij} \delta(\mathbf{k} - \mathbf{k}')$, this transforms into

$$\begin{aligned} \hat{H}_{int}^{(\chi)} = & (2\pi)^{-D/2} \hbar \int \int d^D \mathbf{K} d^D \mathbf{k} \left[\tilde{\chi}_D(\mathbf{k}, \mathbf{K}) \hat{a}_1^\dagger \left(\frac{m_1 \mathbf{K}}{m_1 + m_2} - \mathbf{k} \right) \right. \\ & \left. \times \hat{a}_2^\dagger \left(\frac{m_2 \mathbf{K}}{m_1 + m_2} + \mathbf{k} \right) \hat{a}_3(\mathbf{K}) + \text{H.c.} \right]. \end{aligned} \quad (49)$$

We next assume that the Fourier component $\tilde{\chi}_D(\mathbf{k}, \mathbf{K})$ depends only on \mathbf{k} , and impose a momentum cutoff on $\tilde{\chi}_D(\mathbf{k})$, such that $\tilde{\chi}_D(\mathbf{k})$ vanishes if $|\mathbf{k}| > k_m$ and is a constant, $\tilde{\chi}_D(\mathbf{k}) = \chi_D$, for $|\mathbf{k}| < k_m$.

Similar considerations can be applied to the quartic interaction terms in our Hamiltonian, given by Eq. (4). Because of translational invariance, $\kappa_D^{(ij)}(\mathbf{x}, \mathbf{y}, \mathbf{x}', \mathbf{y}')$ is written as $\kappa_D^{(ij)}(\mathbf{r}, \mathbf{r}', \mathbf{R} - \mathbf{R}')$, where $\mathbf{r} = \mathbf{x} - \mathbf{y}$, $\mathbf{r}' = \mathbf{x}' - \mathbf{y}'$, $\mathbf{R} = (m_i \mathbf{x} + m_j \mathbf{y})/(m_i + m_j)$, and $\mathbf{R}' = (m_i \mathbf{x}' + m_j \mathbf{y}')/(m_i + m_j)$. Transforming to Fourier space, we assume that the Fourier component $\tilde{\kappa}_D^{(ij)}(\mathbf{k}, \mathbf{k}', \mathbf{K})$, where $\mathbf{K} = \mathbf{k} + \mathbf{k}'$, does not depend on \mathbf{K} , and impose a momentum cutoff such that $\tilde{\kappa}_D^{(ij)}(\mathbf{k}, \mathbf{k}') = \kappa_D^{(ij)}$ if $|\mathbf{k}|, |\mathbf{k}'| < k_m$, and is zero otherwise. The final form of the cutoff dependent interaction Hamiltonian can now be written as

$$\begin{aligned} \hat{H}_{int} = & (2\pi)^{-D/2} \hbar \chi_D \int_{|\mathbf{k}|=0}^{k_m} d^D \mathbf{k} \int d^D \mathbf{K} \left[\hat{a}_1^\dagger \left(\frac{m_1 \mathbf{K}}{m_1 + m_2} + \mathbf{k} \right) \right. \\ & \times \hat{a}_2^\dagger \left(\frac{m_2 \mathbf{K}}{m_1 + m_2} - \mathbf{k} \right) \hat{a}_3(\mathbf{K}) + \text{H.c.} \left. \right] + (2\pi)^{-D} \\ & \times \sum_{i,j=1}^3 \frac{\hbar \kappa_D^{(ij)}}{2} \int_{|\mathbf{k}|=0}^{k_m} d^D \mathbf{k} \int_{|\mathbf{k}'|=0}^{k_m} d^D \mathbf{k}' \int d^D \mathbf{K} \\ & \times \hat{a}_i^\dagger \left(\frac{m_i \mathbf{K}}{m_i + m_j} + \mathbf{k} \right) \hat{a}_j^\dagger \left(\frac{m_j \mathbf{K}}{m_i + m_j} - \mathbf{k} \right) \\ & \times \hat{a}_i \left(\frac{m_i \mathbf{K}}{m_i + m_j} + \mathbf{k}' \right) \hat{a}_j \left(\frac{m_j \mathbf{K}}{m_i + m_j} - \mathbf{k}' \right). \end{aligned} \quad (50)$$

The noninteracting part of the Hamiltonian, in terms of $\hat{a}_i(\mathbf{k})$, is

$$\hat{H}_0 = \sum_{i=1}^3 \frac{\hbar^2}{2m_i} \int d^D \mathbf{k} k^2 \hat{a}_i^\dagger(\mathbf{k}) \hat{a}_i(\mathbf{k}) + \hbar \Delta \omega \int d^D \mathbf{k} \hat{a}_3^\dagger(\mathbf{k}) \hat{a}_3(\mathbf{k}). \quad (51)$$

In the case of nonlinear optical interactions, the coupling constants χ_D and $\kappa_D^{(ij)}$ are proportional to the Bloembergen second- and third-order susceptibilities of the nonlinear medium [3,29], while in the case of atomic/molecular BEC interactions the quartic couplings $\kappa_D^{(ij)}$ are related to the s -wave scattering amplitudes [30]. For example, in the diagonal case and in three space dimensions, $\kappa_3^{(ii)}$ is given by $\kappa_3^{(ii)} = 4\pi\hbar a_{ii}/m_i$, where a_{ii} is the s -wave scattering length within the i th species, while the interspecies couplings are $\kappa_3^{(ij)} = \kappa_3^{(ji)} = 2\pi\hbar a_{ij}/\mu_{ij}$, where a_{ij} is the corresponding cross-scattering length and $\mu_{ij} = m_i m_j / (m_i + m_j)$ is the reduced mass [24,30]. The form of the parametric coupling will depend on the particular mechanism that can be used for atomic dimerization, such as Feshbach resonance or Raman photoassociation [31,22]. In addition, we note that in cases where fermionic fields are involved, the corresponding quartic self-interaction terms must be omitted from the Hamiltonian.

B. Exact diboson solutions

We can now analyze the eigenvalue problem $\hat{H}|\varphi_{\mathbf{K}}^{(2)}(k_m)\rangle = E_{\mathbf{K}}^{(2)}(k_m)|\varphi_{\mathbf{K}}^{(2)}(k_m)\rangle$ directly, by considering the two-particle eigenstate in Fourier space:

$$|\varphi_{\mathbf{K}}^{(2)}(k_m)\rangle = \left[\hat{a}_3^\dagger(\mathbf{K}) + (2\pi)^{-D/2} \int_{|\mathbf{k}|=0}^{k_m} d^D \mathbf{k} G(\mathbf{k}) \times \hat{a}_1^\dagger\left(\frac{m_1 \mathbf{K}}{M} + \mathbf{k}\right) \hat{a}_2^\dagger\left(\frac{m_2 \mathbf{K}}{M} - \mathbf{k}\right) \right] |0\rangle, \quad (52)$$

so that the cutoff dependent correlation function is $g(\mathbf{r}, k_m) = \int_{|\mathbf{k}|=0}^{k_m} d^D \mathbf{k} G(\mathbf{k}) \exp(i\mathbf{k} \cdot \mathbf{r}) / (2\pi)^D$.

This implies that, due to the cutoff in the nonlinearities, we need only investigate eigenstates for which $G(\mathbf{k})$ satisfies the equation

$$(k^2 + r_0^{-2})G(\mathbf{k}) = -q, \quad (53)$$

if $|\mathbf{k}| < k_m$ and vanishes for $|\mathbf{k}| > k_m$. The energy eigenvalue $E_{\mathbf{K}}^{(2)}(k_m)$ is given by

$$E_{\mathbf{K}}^{(2)}(k_m) = \frac{\hbar^2 K^2}{2M} - \frac{\hbar^2}{2\mu r_0^2}, \quad (54)$$

where the length scale r_0 is to be found by solving the following eigenvalue equation:

$$r_0^{-2} = \frac{2\mu}{\hbar} [\Delta - \chi_D g(0, k_m)]. \quad (55)$$

Here $k = |\mathbf{k}|$, $K = |\mathbf{K}|$, Δ is given by Eq. (20), while q is defined as

$$q \equiv 2\mu[\chi_D + \kappa_D g(0, k_m)]/\hbar. \quad (56)$$

The above equations represent the Fourier transform equivalent of Eq. (15) and Eq. (18), except that now they are valid for $|\mathbf{k}| < k_m$.

In order to evaluate the soliton binding energy and the effective radius, we solve these equations for $g(0, k_m)$, and obtain

$$g(0, k_m) = -\chi_D \left(\kappa_D + \frac{\hbar r_0^{D-2}}{2\mu f_D(r_0 k_m)} \right)^{-1}. \quad (57)$$

Here the dimensionless cutoff structure function is defined as

$$f_D(r_0 k_m) = \frac{1}{(2\pi)^D} \int_{|\mathbf{x}|=0}^{r_0 k_m} \frac{d^D \mathbf{x}}{1+x^2}, \quad (58)$$

and its explicit form in one, two, and three dimensions ($D = 1, 2, 3$) is given by

$$f_1(r_0 k_m) = \frac{1}{\pi} \tan^{-1}(r_0 k_m), \quad (59)$$

$$f_2(r_0 k_m) = \frac{1}{4\pi} \ln(1 + r_0^2 k_m^2), \quad (60)$$

$$f_3(r_0, k_m) = \frac{1}{2\pi^2} [r_0 k_m - \tan^{-1}(r_0 k_m)]. \quad (61)$$

This result clearly shows the difference caused by the dimensionality of the space. In one dimension $f_1(r_0 k_m)$ approaches a constant value if $k_m \rightarrow \infty$, while in two and three dimensions $f_D(r_0 k_m)$ has a logarithmic or linear divergence, respectively. The effect of this divergence depends on whether or not the additional quartic interaction is present. If it is present (with $\kappa_D > 0$), there are exact solutions without cutoff, and $g(0, k_m \rightarrow \infty) = -\chi_D / \kappa_D$, so that the energy eigenvalue $E_{\mathbf{K}}^{(2)}(k_m \rightarrow \infty)$ takes the form of Eq. (36), and $g(\mathbf{r}) = 0$ if $|\mathbf{r}| > 0$. In other words, the solutions in two and three dimensions have a finite energy (unlike the energy divergence in the nonlinear Schrödinger model with an attractive δ -function potential) but zero radius in the limit of $k_m \rightarrow \infty$. If, however, $\kappa_D \leq 0$, as in the attractive nonlinear Schrödinger model, we must impose a finite cutoff on the couplings to prevent an energy divergence. Simultaneously, a finite cutoff prevents singularities in space.

With a finite cutoff, the eigenvalue problem for $E_{\mathbf{K}}^{(2)}(k_m)$, Eq. (54), reduces to the solution of the following eigenvalue equation:

$$r_0^{-2} = \frac{2\mu}{\hbar} \left[\Delta + (\chi_D)^2 \left(\kappa_D + \frac{\hbar r_0^{D-2}}{2\mu f_D(r_0 k_m)} \right)^{-1} \right], \quad (62)$$

which is Eq. (55) rewritten in terms of the cutoff structure function $f_D(r_0 k_m)$, using $g(0, k_m)$ from Eq. (57). Here r_0 must be real and positive for a localized bound state.

Analysis of this equation, using the explicit results for the cutoff structure functions (59)–(61), shows that under certain conditions a positive solution for r_0 is available. This condition in the cases of one and two dimensions can be written in the form of Eq. (25), while in the three-dimensional case it is modified to $(\chi_3)^2 + \Delta[\kappa_3 + \pi^2 \hbar / (\mu k_m)] > 0$.

In the simplest case of $\kappa_D = 0$ (which can be considered only if the cutoff and the couplings are independent of each other), $\Delta = 0$, and in the limit $k_m \gg r_0^{-1}$ the eigenvalue equation is simplified, and even solved analytically in one- and three-dimensional cases. The resulting radii r_0 and binding energies $E_b^{(2)} = \hbar^2 / (2\mu r_0^2)$ are determined by:

$$\begin{aligned} r_0 &\simeq (\hbar^2 / 2\chi_1^2 \mu^2)^{1/3}, \quad E_b^{(2)} \simeq (\hbar^2 \mu / 2)^{1/3} (\chi_1)^{4/3} \quad (D=1); \\ r_0 &\simeq (\pi / 2)^{1/2} (\hbar / \chi_2 \mu) [\ln(r_0 k_m)]^{-1/2}, \\ E_b^{(2)} &= \hbar^2 / (2\mu r_0^2) \quad (D=2); \\ r_0 &\simeq (\pi \hbar / \chi_3 \mu) (2k_m)^{-1/2}, \\ E_b^{(2)} &\simeq (\chi_3)^2 \mu k_m / \pi^2 \quad (D=3). \end{aligned} \quad (63)$$

Here, in the two-dimensional case, the diboson radius r_0 and the binding energy $E_b^{(2)}$ can easily be found numerically. The one-dimensional result (in the limit of $k_m \gg r_0^{-1}$) reproduces the result of Eqs. (32) and (33) obtained using the cutoff independent treatment.

C. N -particle results: Independent diboson ansatz

To estimate the ground state energy, in the cutoff dependent N -particle problem, we use the following momentum-space ansatz, corresponding to $N/2$ (where we assume N is even) independent dibosons:

$$\begin{aligned} |\tilde{\varphi}_0^{(N)}(k_m)\rangle &= \left(\hat{a}_3^\dagger(0) + (2\pi)^{-D/2} \int_{|\mathbf{k}|=0}^{k_m} d^D \mathbf{k} G(\mathbf{k}) \right. \\ &\quad \left. \times \hat{a}_1^\dagger(\mathbf{k}) \hat{a}_2^\dagger(-\mathbf{k}) \right)^{N/2} |0\rangle. \end{aligned} \quad (64)$$

Operating with the cutoff dependent Hamiltonian on this ansatz we find, for an infinite interaction volume, the following result for the corresponding energy (see Appendix B):

$$\tilde{E}_0^{(N)}(k_m) = \frac{N}{2} E_0^{(2)}(k_m), \quad (65)$$

where $E_0^{(2)}(k_m)$ is determined by Eqs. (54) and (62). This result represents an upper bound to the ground state energy, and is no longer the exact solution unless $k_m \rightarrow \infty$. It is expressed in terms of the energy $E_0^{(2)}(k_m)$ of individual dibosons, and depends only on the parametric coupling χ_D and the quartic cross-coupling κ_D . The contribution of the other quartic terms, including the self interaction $\sim \kappa_D^{(33)}$ of the $\hat{\Psi}_3$

field, is negligible since we have used a free space expansion of $\hat{\Psi}_i(\mathbf{x})$ in terms of $\hat{a}_i(\mathbf{k})$. This means that the result for $\tilde{E}_0^{(N)}(k_m)$ corresponds to an infinite volume or zero particle density, where the contributions due to the quartic interactions other than the κ_D coupling (which affects the binding within individual dibosons) vanish.

The lower bound in this cutoff dependent N -particle problem can also be estimated following previous methods. Since the previous cutoff independent result was obtained by ignoring kinetic energy terms, the lower bound is unchanged from the previous section, Eq. (43). Consequently, for the true cutoff dependent ground state energy $E_0^{(N)}(k_m)$ we have now the result that

$$E_l^{(N)} = \frac{N}{2} E_0^{(2)} \leq E_0^{(N)}(k_m) \leq \tilde{E}_0^{(N)}(k_m) = \frac{N}{2} E_0^{(2)}(k_m), \quad (66)$$

where $E_l^{(N)} \neq \tilde{E}_0^{(N)}(k_m)$, unless $k_m \rightarrow \infty$.

Thus, with a finite cutoff the ansatz corresponding to $N/2$ independent dibosons no longer gives the energy coinciding with the lower bound, and only provides an upper bound to the ground state energy. In other words, it is no longer the exact eigenstate and therefore does not necessarily result in the lowest possible energy.

D. N -particle results: Coherent variational ansatz

The second type of ansatz that we employ here is the coherent or mean-field theory (MFT) ansatz:

$$|\tilde{\varphi}_c^{(N)}\rangle = \exp\left(\int d^3 \mathbf{x} \sum_{i=1}^3 \psi_i(\mathbf{x}) \hat{\Psi}_i^\dagger(\mathbf{x})\right) |0\rangle. \quad (67)$$

The coherent ansatz is equivalent to a mean-field theory description of the system, where the operators are replaced by their mean values and a factorization is assumed. It is an approximate (semiclassical) eigenstate that describes three coupled fields at large N , under broken symmetry conditions. Compared with the previous case of the $N/2$ independent diboson ansatz, the coherent ansatz can provide a lower energy at large N and for certain parameter values. To show this, we use a variational approach and choose trial functions $\psi_i(\mathbf{x})$ in the form of Gaussians, assuming in addition that $\psi_1(\mathbf{x}) = \psi_2(\mathbf{x})$:

$$\begin{aligned} \psi_1(\mathbf{x}) = \psi_2(\mathbf{x}) &= g_1 \exp[-|\mathbf{x}|^2 / (2w_1^2)], \\ \psi_3(\mathbf{x}) &= -g_3 \exp[-|\mathbf{x}|^2 / (2w_3^2)]. \end{aligned} \quad (68)$$

Here g_i and w_i are regarded as free variational parameters, the negative sign for $\psi_3(\mathbf{x})$ is to ensure that the coupling energy is negative for $\chi_D > 0$, and the normalization implies that the Gaussian parameters must satisfy $2\pi^{3/2}[g_1^2 w_1^3 + g_3^2 w_3^3] = N$. We will assume that the coherent ansatz is slowly varying such that the Gaussian width scales are much larger than k_m^{-1} , allowing the momentum cutoff to be neglected. Substituting these trial functions into the Hamil-

tonian (1), (2), and (5), we find that the corresponding variational energy $\tilde{E}_c^{(N)}$, in two and three space dimensions, is given by

$$\begin{aligned} \tilde{E}_c^{(N)} = & \left(\frac{\pi}{2} \right)^{D/2} \left(\frac{2^{(D-2)/2} D \hbar^2}{2\mu} g_1^2 w_1^{D-2} \right. \\ & + \frac{2^{(D-2)/2} D \hbar^2}{2m_3} g_3^2 w_3^{D-2} + 2^{D/2} \hbar \Delta \omega g_3^2 w_3^D \\ & - \frac{2^{D+1} \hbar \chi_D g_1^2 g_3^2 w_1^D w_3^D}{(w_1^2 + 2w_3^2)^{D/2}} + \hbar \left(\kappa_D + \frac{\kappa_D^{(11)}}{2} + \frac{\kappa_D^{(22)}}{2} \right) g_1^4 w_1^D \\ & + \frac{\hbar \kappa_D^{(33)}}{2} g_3^4 w_3^D \\ & \left. + \frac{2^{D/2} \hbar (\kappa_D^{(13)} + \kappa_D^{(23)}) g_1^2 g_3^2 w_1^D w_3^D}{2(w_1^2 + w_3^2)^{D/2}} \right) \quad (D=2,3). \quad (69) \end{aligned}$$

The result of minimization of $\tilde{E}_c^{(N)}$, under the constraint of $2\pi^{3/2}[g_1^2 w_1^3 + g_3^2 w_3^3] = N$, is considerably simplified in the region where the parametric coupling is dominant and N is not too large, so that one can neglect the terms due to $\Delta \omega$ and the quartic couplings $\kappa_D^{(ij)}$. In this region, and for $m_3 = m_1 + m_2$ and $m_1 = m_2$ (so that $m_3 = 4\mu$), we obtain the MFT minimum energy of

$$\tilde{E}_c^{(N)} = -A_D N^{(6-D)/(4-D)} \left(\frac{\hbar^2}{2\mu} \right) \left(\frac{2\mu \chi_D}{\hbar} \right)^{4/(4-D)} \quad (D=2,3), \quad (70)$$

where A_D is a dimensionless constant given by $A_2 \approx 7.42 \times 10^{-3}$ in two dimensions, and by $A_3 \approx 1.2 \times 10^{-5}$ in three dimensions. The energy $\tilde{E}_c^{(N)}$ scales as N^2 in two dimensions, and as N^3 in the three-dimensional case. Comparing this with the linear dependence on N of the energy estimate $\tilde{E}_0^{(N)}(k_m)$ from the independent diboson ansatz, Eq. (65), we conclude that there exists a crossover or a critical boson number N_{cr} beyond which (i.e., for $N > N_{cr}$) the coherent variational ansatz becomes more favorable, as $\tilde{E}_c^{(N)} < \tilde{E}_0^{(N)}(k_m)$. The value of N_{cr} is easily found using the above simple result for $\tilde{E}_c^{(N)}$ which neglects the role of the quartic couplings so that all parameter dependences are explicit. For nonzero quartic couplings, the dependence of the minimum energy $\tilde{E}_c^{(N)}$ is no longer given by such a simple expression. The minimization does not reveal explicit scaling properties similar to those in Eq. (70) and it must be carried out for different values of N independently. This is further analyzed in Sec. VI as applied to parameter values characteristic of BEC interactions.

To conclude our discussion of the results in the case of pure parametric interactions, we note that for the symmetric case under consideration, i.e., for $\psi_1(\mathbf{x}) = \psi_2(\mathbf{x})$, the system can be formally reduced to the model of degenerate parametric interaction which is known to support higher-dimensional classical solitons [15–17]. Thus, together with providing a minimum energy to the classical Hamiltonian, the above co-

herent variational ansatz gives optimum Gaussian parameters which correspond to the approximate analytical form of classical solitons in this pure parametric case, in two and three space dimensions. The optimum length scales corresponding to soliton widths (for $\Delta \omega = 0$, $m_1 = m_2$, and $m_3 = m_1 + m_2$) are nearly identical for the three fields and are given by $w_1 = w_2 \approx 1.2 \times 10^2 N^{-1} (2\mu \chi_3 / \hbar)^{-2}$ and $w_3 \approx 0.88 w_1$, in three space dimensions. The corresponding values of the field amplitudes are determined by

$$g_1 = g_2 \approx 1.7 \times 10^{-4} N^2 (2\mu \chi_3 / \hbar)^3$$

and $g_3 \approx 1.1 g_1$. These, in turn, give the following relation for the average number of particles $[\bar{N}_i = \int d^3 \mathbf{x} |\psi_i(\mathbf{x}, t)|^2]$ present in the fields $\psi_{1,2}$ and ψ_3 : $\bar{N}_{1,2} / \bar{N}_3 \approx 1.21$. In two dimensions, the parametric soliton optimum widths and amplitudes are given by

$$w_1 = w_2 \approx 6.98 N^{-1/2} (2\mu \chi_2 / \hbar)^{-1},$$

$$w_3 \approx 0.86 w_1,$$

$$g_1 = g_2 \approx 4.06 \times 10^{-2} N (2\mu \chi_2 / \hbar),$$

and $g_3 \approx 1.05 g_1$, yielding $\bar{N}_{1,2} / \bar{N}_3 \approx 1.24$. Clearly the soliton width must be much larger than k_m^{-1} for our use of the cutoff independent Hamiltonian to be justified.

V. PHYSICAL APPLICATIONS: PHOTONIC INTERACTIONS

An important application of the results of our parametric field theory is in optics, where it describes the nonlinear optical process of frequency conversion or sum-frequency generation. Here the parametric coupling χ_D is due to the second-order nonlinearity of a nonlinear medium, while the $\kappa_D^{(ij)}$ terms are due to self- and cross-phase modulation. Straightforward application of the previous results is, however, prevented by the fact that the noninteracting Hamiltonian \hat{H}_0 for the propagating light fields is in general different from Eq. (2). It is defined in a moving reference frame and is asymmetric with respect to the longitudinal (direction of propagation) and transverse directions [15,29]:

$$\begin{aligned} \hat{H}_0 = & \int d^D \mathbf{x} \left[\sum_{i=1}^3 \left(\frac{\hbar^2}{2m_{i\parallel}} |\nabla_{\parallel} \hat{\Psi}_i|^2 + \frac{\hbar^2}{2m_{i\perp}} |\nabla_{\perp} \hat{\Psi}_i|^2 \right) \right. \\ & \left. + \hbar \Delta \omega \hat{\Psi}_3^{\dagger} \hat{\Psi}_3 \right]. \quad (71) \end{aligned}$$

Here $\hat{\Psi}_{1,2}$ and $\hat{\Psi}_3$ represent three optical fields with carrier wave numbers $\mathbf{k}_{1,2}$, $\mathbf{k}_3 = \mathbf{k}_1 + \mathbf{k}_2$ and frequencies $\omega_i = \omega(k_i)$ ($i = 1, 2, 3$), while $\Delta \omega = \omega_3 - (\omega_1 + \omega_2)$ is the phase mismatch. The longitudinal coordinate (x_{\parallel}) is defined in a moving frame, $x_{\parallel} = x_L - vt$, where x_L is the laboratory frame coordinate and $v = \partial \omega_i / \partial k$ is the group velocity, which is assumed equal at all three carrier frequencies. In addition, $m_{i\parallel} = \hbar / \omega_i''$ are effective longitudinal masses due to the group

velocity dispersion, where $\omega_i'' = \partial^2 \omega_i / \partial k^2$ is the dispersion coefficient in the i th frequency band. The transverse masses $m_{i\perp} = \hbar \omega_i / v^2$ are caused by diffraction, and the corresponding term in \hat{H}_0 is only relevant in two and three dimensions. The coupling constants χ_D and $\kappa_D^{(ij)}$ in the interaction Hamiltonian are proportional to the Bloembergen second- and third-order nonlinear susceptibilities ($\chi_B^{(2)}$ and $\chi_B^{(3)}$ [32]) of the nonlinear medium, respectively [3,14,29]:

$$\chi_D \approx \frac{\chi_B^{(2)}}{n^3} \left(\frac{\hbar \omega_1 \omega_2 \omega_3}{2 \varepsilon_0} \right)^{1/2} \frac{1}{d^{(3-D)/2}}, \quad \kappa_D \approx \frac{3 \hbar \chi_B^{(3)} \omega_1 \omega_2}{4 \varepsilon_0 n^4 d^{3-D}}, \quad (72)$$

where n is the refractive index, which we assume is nearly the same at all three frequencies, and d is the effective modal (waveguide) diameter.

Our treatment here is similar to a previous theory of degenerate optical parametric interaction [11], except that the present nondegenerate theory has an additional degree of freedom due to the fact that the low-frequency fields (Ψ_1 and Ψ_2) are different. In practical terms, this gives the possibility of employing either type I or type II phase matching, i.e., the fields can be different either in frequencies or in polarization, or else in both.

A. Analytic results

The asymmetric form of the noninteracting Hamiltonian does not qualitatively change the results of the previous sections. The results are, however, modified quantitatively in two and three dimensions. Omitting the details of the derivation we give only the final expressions for the two-particle eigenvalue problem and the simplest diphoton solutions.

First we mention that in one dimension the results of the earlier sections are unchanged, with the understanding that the effective masses m_i are interpreted as dispersive ones, $m_i \equiv m_{i\parallel}$. In two and three dimensions, the two-particle or diphoton energy is determined by

$$E_{\mathbf{K}}^{(2)}(k_m) = \frac{\hbar^2}{2} \left(\frac{K_{\parallel}^2}{M_{\parallel}} + \frac{K_{\perp}^2}{M_{\perp}} \right) - \frac{\hbar^2}{2 \mu_{\parallel} r_0^2}, \quad (73)$$

where r_0 is to be found by solving the following eigenvalue equation:

$$r_0^{-2} = \frac{2 \mu_{\parallel}}{\hbar} \left[\Delta + (\chi_D)^2 \left(\kappa_D + \frac{\hbar r_0^{D-2}}{2 \mu_{\parallel} f_D(r_0 k_m, \mu_r)} \right)^{-1} \right]. \quad (74)$$

Here the diphoton momentum \mathbf{K} is decomposed into longitudinal and transverse components so that $K^2 \equiv |\mathbf{K}|^2 = K_{\parallel}^2 + K_{\perp}^2$. In addition, we have introduced the longitudinal and transverse reduced masses $\mu_{\parallel} \equiv m_{1\parallel} m_{2\parallel} / (m_{1\parallel} + m_{2\parallel})$ and $\mu_{\perp} \equiv m_{1\perp} m_{2\perp} / (m_{1\perp} + m_{2\perp})$, and have defined $M_{\parallel} \equiv m_{1\parallel} + m_{2\parallel}$, $M_{\perp} \equiv m_{1\perp} + m_{2\perp}$, and $\mu_r \equiv \mu_{\perp} / \mu_{\parallel}$. The cutoff structure function $f_D(r_0 k_m, \mu_r)$ is defined as

$$f_D(r_0 k_m, \mu_r) = \frac{1}{(2\pi)^D} \int_{|\mathbf{x}|=0}^{r_0 k_m} \frac{d^D \mathbf{x}}{1 + x_{\parallel}^2 + x_{\perp}^2 / \mu_r} \quad (D=2,3), \quad (75)$$

and the effective detuning Δ is now given by

$$\Delta \equiv \frac{\hbar}{2} \left(\frac{K_{\parallel}^2}{M_{\parallel}} + \frac{K_{\perp}^2}{M_{\perp}} \right) - \frac{\hbar}{2} \left(\frac{K_{\parallel}^2}{m_{3\parallel}} + \frac{K_{\perp}^2}{m_{3\perp}} \right) - \Delta \omega. \quad (76)$$

In the limit of $k_m \rightarrow \infty$, which corresponds to the simplified cutoff independent treatment, one can again arrive at the same conclusions as in Sec. III on the pointlike structure of the multidimensional two-particle bound states. The cutoff dependent results are modified due to the dependence of the cutoff structure function (75) on the relation $\mu_r = \mu_{\perp} / \mu_{\parallel}$. The integrations in $f_D(r_0 k_m, \mu_r)$ cannot be carried out as easily as in the symmetric case of Sec. IV corresponding to $\mu_r = 1$. Instead, for arbitrary values of μ_r , the integrals and the resulting binding energies can be evaluated numerically. If, however, $\sqrt{\mu_r} \ll 1$ and $r_0 k_m \gg 1$ one can obtain the following approximate results:

$$f_2(r_0 k_m, \mu_r) \approx \frac{\sqrt{\mu_r}}{2\pi} \ln(2 r_0 k_m), \quad (77)$$

$$f_3(r_0 k_m, \mu_r) \approx \frac{\mu_r r_0 k_m}{2\pi^2} (1 - \ln \sqrt{\mu_r}). \quad (78)$$

With these functions and for $\kappa_D > 0$, the condition (25) of having a positive solution for r_0 in the eigenvalue equation (74) remains unchanged in two dimensions, while in three dimensions it is transformed into

$$(\chi_3)^2 + \Delta \{ \kappa_3 + \pi^2 \hbar / [\mu_{\parallel} \mu_r k_m (1 - \ln \sqrt{\mu_r})] \} > 0, \quad (79)$$

with Δ given by Eq. (76) in both cases.

B. Diphoton binding energies for pure parametric case

In the case of $\kappa_D = 0$ and $\Delta = 0$ Eqs. (73), (74) and (77), (78), together with the earlier one-dimensional result (where we replace μ by μ_{\parallel}), lead to the following simple expressions for the diphoton soliton radii r_0 and the binding energies $E_b^{(2)} = \hbar^2 / (2 \mu_{\parallel} r_0^2)$:

$$\begin{aligned} r_0 &\approx (\hbar^2 / 2 \chi_1^2 \mu_{\parallel}^2)^{1/3}, \quad E_b^{(2)} \approx (\hbar^2 \mu_{\parallel} / 2)^{1/3} (\chi_1)^{4/3} \quad (D=1); \\ r_0 &\approx (\pi / 2)^{1/2} (\hbar / \chi_2 \mu_{\parallel}) \mu_r^{-1/4} [\ln(2 r_0 k_m)]^{-1/2}, \\ E_b^{(2)} &\approx \hbar^2 / (2 \mu_{\parallel} r_0^2) \quad (D=2); \\ r_0 &\approx (\pi \hbar / \chi_3 \mu_{\parallel}) (2 \mu_r k_m)^{-1/2} (1 - \ln \sqrt{\mu_r})^{-1/2}, \\ E_b^{(2)} &\approx (\chi_3)^2 \mu_{\parallel} \mu_r k_m (1 - \ln \sqrt{\mu_r}) / \pi^2 \quad (D=3). \end{aligned} \quad (80)$$

To illustrate how large a binding energy might be obtained we consider parameter values characteristic of highly nonlinear parametric materials, such as GaAs asymmetric quantum well structures [33]. We note, however, that these

types of materials often have practical limitations involving restricted wavelengths, lack of phase matching, or high absorption. For example, high values of $\chi_B^{(2)}$ (up to $\sim 9 \times 10^{-7}$ m/V) observed in the GaAs case were only around the fundamental (subharmonic) wavelength of about $\lambda_1 \sim 9.2$ μm , and the absorption was high. Other candidates such as organic materials [34] have the advantage of operating at shorter wavelength ($\lambda_1 \sim 1.3$ μm), but the values of $\chi_B^{(2)}$ are smaller ($\chi_B^{(2)} \sim 10^{-10}$ m/V). Other factors and requirements that may have practical importance are similar to those discussed in Ref. [11] for the case of degenerate parametric interaction.

For the present nondegenerate parametric interaction, we summarize the estimates of the diphoton radii and binding energies by considering reference parameter values similar to those of GaAs. These are chosen as follows: $\chi_B^{(2)} = 9 \times 10^{-7}$ m/V, $\lambda_1 = 9.2$ μm , and $n = 3.3$. In addition, we assume that $\omega_1 \approx \omega_2 \approx \omega_3/2$ ($\lambda_1 \approx \lambda_2 \approx 2\lambda_3$), resulting in $\mu_\perp = 1.3 \times 10^{-36}$ kg, and we choose the dispersion coefficients $\omega'_1 \approx \omega'_2$ such that $\mu_r = \mu_\perp / \mu_\parallel = 0.01$. The waveguide diameter d required to evaluate the value of the coupling constant $\chi_D = \chi_3 d^{(D-3)/2}$ ($D=1,2$) in one and two dimensions is chosen as $d = 5\lambda_1$. Finally, for the cutoff dependent two- and three-dimensional cases, we choose the cutoff at the inverse of the longest wavelength $k_m = 2\pi/\lambda_1$, while in the one-dimensional case the cutoff dependences can be neglected as long as $r_0 k_m \gg 1$.

With these parameter values, the resulting radii r_0 and binding energies $E_b^{(2)}$ of the parametric diphotons are given in the following table

| | Coupling χ_D | r_0 (μm) | $E_b^{(2)}$ (eV) |
|-------|---|-------------------------|----------------------|
| $D=1$ | 5.4×10^6 ($\text{m}^{1/2}/\text{s}$) | 22 | 5.3×10^{-7} |
| $D=2$ | 3.7×10^4 (m/s) | 43 | 1.4×10^{-7} |
| $D=3$ | 2.5×10^2 ($\text{m}^{3/2}/\text{s}$) | 47 | 1.2×10^{-7} |

(81)

indicating that we expect the higher-dimensional quantum solitons to be less strongly bound and of larger radius than their one-dimensional counterparts.

Thus we have shown that nondegenerate parametric interactions can provide diphoton bound states in one, two, and three space dimensions. The diphoton has the form of a quantum superposition of two states one of which contains a photon of the sum-frequency field $\hat{\Psi}_3$, while the other involves a pair of photons of the lower-frequency fields $\hat{\Psi}_1$ and $\hat{\Psi}_2$. The diphoton can be viewed as a photonic analog of a two-quark state model of mesons, and be termed, as in the case of degenerate parametric interaction [14], an ‘‘optical meson.’’ The relatively large binding energy, as compared to quantum solitons based on $\chi^{(3)}$ nonlinearities [21], combined with low-temperature experimental techniques, could make it feasible to observe this simple quantum soliton in experiment.

VI. BEC INTERACTIONS

Another example of a physical system that can be treated by the Hamiltonian (1),(2), and (5) or (50) is a coupled atomic/molecular BEC. Here the parametric coupling represents the coherent process of formation of dimer molecules ($\hat{\Psi}_3$ field) from pairs of atoms ($\hat{\Psi}_1$ and $\hat{\Psi}_2$ fields) either of distinct atomic species, or in distinct quantum states. In the case of degenerate parametric interaction this has been considered in Refs. [19,22,23,35,36]. Here we extend the basic results to the case of nondegenerate parametric interaction, i.e., to three coupled Bose condensates, thus extending the variety of ultracold molecular gases that could be created via BEC interactions.

In this directly applicable case of BEC interactions, $m_{1,2}$ and $m_3 = m_1 + m_2 = M$ are the atomic and molecular masses, the coupling constant χ_D is related to the molecular formation rate, while $\kappa_D^{(ij)}$ are the effective intra- and interspecies couplings due to s -wave scattering amplitudes a_{ij} [24,30]. In addition, $\hbar\Delta\omega$ is the bare formation energy of the molecular species. Physical mechanisms that can realize coherent atomic dimerization and produce ultracold molecules include Feshbach resonance and Raman photoassociation [31,35]. Feshbach resonances have already been observed [37], while experiments of this type with Raman photoassociation are under way [39] in the case of single-species (degenerate) atomic BEC, the theory of which is given elsewhere [22].

The simplest nontrivial objects in such coupled atomic/molecular BEC systems that can be described by our theory, are two-particle (diboson) quantum solitons in three dimensions ($D=3$), i.e. ‘‘dressed’’ molecules, each of which exists in a superposition with a pair of atoms. With a characteristic χ_3 value estimate of about $\chi_3 \approx 10^{-6}$ $\text{m}^{3/2}/\text{s}$ [35,39,22], the atomic masses $m_1 = m_2 \approx 10^{-25}$ kg, and assuming that the s -wave scattering length $a_{12} \approx 5$ nm, so that $\mu = m_1/2 \approx 0.5 \times 10^{-25}$ kg and $\kappa_3 = 2\pi\hbar a_{12}/\mu \approx 6.6 \times 10^{-17}$ m^3/s , Eq. (36) results in a quantum soliton binding energy of $E_b^{(2)} = -E_0^{(2)} = \hbar(\chi_3)^2/\kappa_3 \approx 10^{-11}$ eV, for $\Delta\omega=0$. This is the result of the idealized quantum theory without a momentum cutoff (i.e., $k_m \rightarrow \infty$), which strictly speaking cannot be applied in a self-consistent way to BEC interactions with a nonzero value of κ_3 .

If we include the effect of momentum cutoffs and assume that the scattering length a_{12} provides a natural cutoff at $k_m \approx 2\pi/a_{12}$, then $k_m \approx 4\pi^2\hbar/(\kappa_3\mu)$. In this case the energy $E_0^{(2)}(k_m)$ is found from Eqs. (54) and (62) where the cutoff structure function $f_3(r_0 k_m)$ is given by Eq. (61), with $k_m \approx 4\pi^2\hbar/(\kappa_3\mu)$. For $\Delta\omega=0$ and assuming $k_m r_0 \gg 1$, this gives

$$E_0^{(2)}(k_m) \approx -4\hbar(\chi_3)^2/(5\kappa_3). \quad (82)$$

The resulting binding energy $E_b^{(2)}(k_m) = -E_0^{(2)}(k_m)$ and the corresponding radius $r_0 = \hbar(2\mu E_b^{(2)})^{-1/2}$, for the parameter values as above and $k_m \approx 2\pi/a_{12} = 1.26$ nm^{-1} , are $E_b^{(2)}(k_m) = 0.8 \times 10^{-11}$ eV and $r_0 = 0.3$ μm . Thus, the binding energy with momentum cutoff is very close to the idealized result from Eq. (36), and its magnitude is comparable to achievable temperatures in current BEC experiments.

To give the simplest treatment of coupled atomic/molecular BEC systems, we neglect any loss processes such as three-body inelastic collisions. This may not be easy to realize in practice and will depend on the particular mechanism for atom-molecule coupling. For example, in the case of a Feshbach resonance that couples pairs of atoms to a quasibound excited molecular state, losses due to inelastic atom-molecule collisions can occur at a significant rate [38]. This is clearly a disadvantage that reduces the condensate lifetime. The Raman photoassociation mechanism is, in this sense, more promising [22]. Here the free-bound Raman transitions are induced by two laser fields that couple pairs of atoms to a bound molecular state through excited intermediate states. This has the advantage that one can tune the coupling to a deeply bound molecular state, in which case the rate of inelastic collisions can be significantly reduced [39]. The losses due to collisions with the molecules in the intermediate (virtual) excited states and those due to spontaneous emission can also be reduced by operating in an off-resonance regime with respect to the excited levels.

A. Quantum gas to “liquid” transition

Of more importance than the simplest two-particle bound states are N -particle eigenstates and the ground state energy of this quantum many-body system, in three space dimensions. While this is a difficult problem, some important conclusions can be made by comparing the results obtained with (i) the ansatz of Sec. III E and IV C, corresponding to $N/2$ independent dibosons, and (ii) the coherent ansatz employed in Sec. IV D.

As discussed in Sec. III and IV, a remarkable result that emerges with the treatment of the first type of ansatz is that, in the limit $k_m \rightarrow \infty$ and for $\kappa_3^{(33)} = 0$, it turns into an *exact* eigenstate and provides the exact ground state energy given by Eq. (47). The ground state energy has no lower bound as $\kappa_3 \rightarrow 0$. This is in contrast to the mean-field behavior corresponding to the classical Hamiltonian energy, which is known to have a rigorous lower bound and to support classical solitons [15]. For the case of nonzero κ_3 , this idealized result serves as a lower bound to the true ground state energy with a finite momentum cutoff. For a finite cutoff $k_m \approx 2\pi/a_{12} = 4\pi^2\hbar/(\kappa_3\mu)$, the ansatz corresponding to $N/2$ independent dibosons is no longer the exact eigenstate, and therefore does not necessarily result in the lowest possible energy. The corresponding estimate of the energy in three dimensions is obtained from Eqs. (65) and (82), for $\Delta\omega \rightarrow 0$ and $k_m r_0 \gg 1$:

$$\tilde{E}_0^{(N)}(k_m = 2\pi/a_{12}) \approx -2N\hbar(\chi_3)^2/(5\kappa_3). \quad (83)$$

This corresponds to a low-density regime of a quantum gas of $N/2$ independent dibosons or “dressed” molecules.

We next address the question of whether the coherent or MFT variational ansatz can give a minimum energy $\tilde{E}_c^{(N)}$, from Eq. (69), that is lower than $\tilde{E}_0^{(N)}(k_m)$. This would correspond to a liquidlike regime of coupled Bose condensates, where formation of stable localized wave forms or matter-wave solitons is more energetically favorable than “evapo-

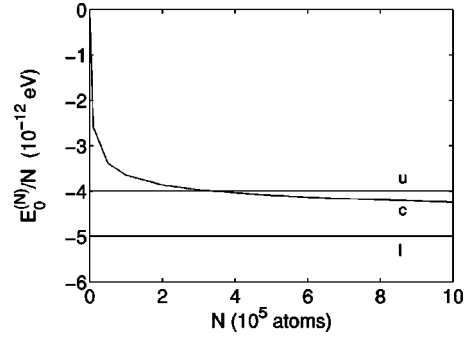


FIG. 1. Estimates for the ground state energy per particle $E_0^{(N)}/N$ as a function of N for $\chi_3 = 10^{-6} \text{ m}^{3/2}/\text{s}$, $m_1 = m_2 = 10^{-25} \text{ kg}$ (so that $\mu = m_1/2 = 0.5 \times 10^{-25} \text{ kg}$ and $m_3 = 2m_1 = 4\mu = 2 \times 10^{-25} \text{ kg}$), and $\Delta\omega = 0$. The upper (u) and lower (l) bounds are for $\kappa_3 = 6.6 \times 10^{-17} \text{ m}^3/\text{s}$ obtained with $a_{12} = 5 \text{ nm}$, and the cutoff for (u) is $k_m = 2\pi/a_{12} \approx 1.26 \text{ nm}^{-1}$. Curve c corresponds to the coherent variational ansatz and represents the minimum energy $\tilde{E}_c^{(N)}$ for the case of $\kappa_3^{(11)} = \kappa_3^{(22)} = 0$, together with $\kappa_3^{(33)} = \kappa_3^{(13)} = \kappa_3^{(23)} = 0$.

ration” into a low-density gas of dibosons or “dressed” molecules. To answer this question in the general case of arbitrary values of the relevant parameters is a difficult problem. Additional complications emerge from the need to analyze stability properties of the actual soliton dynamics, with both parametric and repulsive quartic couplings. It is clear that strong quartic repulsion terms destabilize soliton propagation. If, however, these couplings are not too strong compared to the parametric coupling, then the parametric interaction can still act as a “glue” and compensate the interparticle repulsion, so that stable soliton propagation may occur.

To proceed with our analysis we note that s -wave scattering amplitudes for atom-molecule and molecule-molecule collisional processes are currently not well known. For this reason and for simplicity we neglect the corresponding couplings ($\kappa_3^{(33)} = \kappa_3^{(13)} = \kappa_3^{(23)} = 0$) compared to the atom-atom couplings κ_3 , $\kappa_3^{(11)}$, and $\kappa_3^{(22)}$. In addition, we note that employing the symmetric Gaussian ansatz $\psi_1(\mathbf{x}) = \psi_2(\mathbf{x})$ can only be justified if $\kappa_3^{(11)} = \kappa_3^{(22)}$. We restrict our analysis to the cases where (i) the atomic self-interactions due to $\kappa_3^{(11)}$ and $\kappa_3^{(22)}$ are negligible compared to the cross-interaction κ_3 , so that we can set $\kappa_3^{(11)} = \kappa_3^{(22)} = 0$; (ii) the atomic self- and cross-couplings are all equal to each other, i.e., $\kappa_3^{(11)} = \kappa_3^{(22)} = 2\kappa_3$.

The result of minimization of the variational energy $\tilde{E}_c^{(N)}$, Eq. (69), in case (i) is given in Fig. 1 (curve c , where we plot the estimates for the ground state energy per particle $E_0^{(N)}/N$ versus N). The horizontal line (l) represents the lower bound to the energy given by the idealized solution $E_l^{(N)}/N = -\hbar(\chi_3)^2/(2\kappa_3)$, Eq. (47), while the line u is an upper bound $\tilde{E}_0^{(N)}(k_m)/N$ obtained with the cutoff dependent ansatz corresponding to a low-density regime of a quantum gas of $N/2$ independent dibosons, Eq. (83). The coherent or MFT ansatz gives a lower energy than the diboson ansatz for $N > N_{cr} \approx 3.5 \times 10^5$, so that transition to a liquidlike regime of local-

ized BEC solitons is more favorable in this domain. The relative number of particles in the atomic and molecular solitons $\bar{N}_{1,2}/\bar{N}_3$, obtained from the optimum values of the Gaussian parameters, decreases as N increases, implying that the coupled condensates stabilize against the interatomic repulsions by converting a larger fraction of atoms into molecules. For example, for the total number of particles $N = 10^6$, this fraction is given by $\bar{N}_{1,2}/\bar{N}_3 \approx 0.08$.

In case (ii), we find that $\bar{E}_c^{(N)}$ stays above the value of $\bar{E}_0^{(N)}(k_m)$ for all N and no crossover occurs, implying that the regime of a low-density quantum gas of independent dibosons is always lower in energy than the coupled soliton regime.

Thus, at low particle density, the formation of individual “dressed” molecules (dibosons) is favored, as atoms couple to molecules in a *particlelike* way. These dressed states have interesting properties, reminiscent of Cooper pairs, but cannot be described by the classical parametric soliton equations. At large density (but not too large so that *s*-wave scattering is dominant) and for parameter values characteristic of the case (i), the coherent coupling of three entire condensates is dominant. With large enough parametric coupling, and provided other recombination processes are negligible, there are coherent nonlinear *wavelike* interactions between the atomic and the molecular Bose condensates (just as in nonlinear optics), which make it possible to form stable three-dimensional BEC solitons. For large *s*-wave scattering, case (ii) illustrates a classically stable soliton that is unstable against “evaporation” to a quantum gas of dibosons.

As mentioned earlier, loss processes can be detrimental to the above properties of coupled condensates. In practical terms, the time scale for inelastic losses must be much longer than the coupled condensate formation time scale. We have not given any experimental technique for generating the coupled condensate in its ground state. However, a possible method is to employ evaporative cooling while the atom-molecule coupling is switched on.

B. Coherent BEC soliton dynamics

In performing experiments on coupled atom/molecular BECs, the first signature of the nonlinear interactions we are interested in is likely to be in the dynamical behavior of the coupled condensates. This also allows us to check the stability, at the mean-field level, of the coherent soliton ansatz. We therefore consider $(3D+1)$ spatiotemporal dynamics of the coupled condensates, obtained by direct numerical simulation of the MFT equations for the field amplitudes $\psi_i(t, \mathbf{x})$. These are modified Gross-Pitaevskii equations of the form

$$\begin{aligned} i \frac{\partial \psi_j}{\partial t} = & -\frac{\hbar}{2m_1} \nabla^2 \psi_j + \chi_3 \psi_3 \psi_{3-j}^* + \kappa_3 |\psi_{3-j}|^2 \psi_j \\ & + \kappa_3^{(jj)} |\psi_j|^2 \psi_j + \kappa_3^{(j3)} |\psi_3|^2 \psi_j \quad (j=1,2), \\ i \frac{\partial \psi_3}{\partial t} = & -\frac{\hbar}{2m_3} \nabla^2 \psi_3 + \Delta \omega \psi_3 + \chi_3 \psi_1 \psi_2 + \kappa_3^{(33)} |\psi_3|^2 \psi_3 \\ & + (\kappa_3^{(13)} |\psi_1|^2 + \kappa_3^{(23)} |\psi_2|^2) \psi_3, \end{aligned} \quad (84)$$

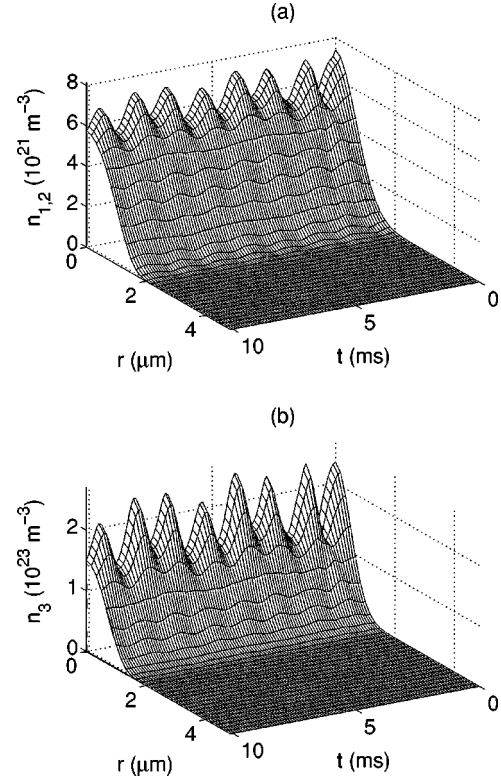


FIG. 2. Mean-field densities $n_{1,2} = |\phi_{1,2}(\mathbf{x}, t)|^2$ and $n_3 = |\phi_3(\mathbf{x}, t)|^2$, representing simultaneous atomic (a) and molecular (b) solitary waves, as depending on time t and the radial coordinate $r = |\mathbf{x}|$ for $\bar{\kappa} = 6.6 \times 10^{-17} \text{ m}^3/\text{s}$ ($\kappa_3 = 6.6 \times 10^{-17} \text{ m}^3/\text{s}$, $\kappa_3^{(11)} = \kappa_3^{(22)} = 0$), $\kappa_3^{(33)} = \kappa_3^{(13)} = \kappa_3^{(23)} = 0$, $m_1 = m_2 = 10^{-25} \text{ kg}$, $\chi_3 = 10^{-6} \text{ m}^3/\text{s}$, and $N = 10^6$. The initial optimum Gaussian parameters are $g_1 = g_2 = 8.6 \times 10^{10} \text{ m}^{-3/2}$, $g_3 = 4.8 \times 10^{10} \text{ m}^{-3/2}$, $w_1 = w_2 = 0.97 \text{ } \mu\text{m}$, and $w_3 = 0.71 \text{ } \mu\text{m}$.

where we recall that $\kappa_3 = (\kappa_3^{(12)} + \kappa_3^{(21)})/2 = \kappa_3^{(12)}$.

We consider for simplicity the symmetric case of $\psi_1(\mathbf{x}) = \psi_2(\mathbf{x})$, with $\kappa_3^{(11)} = \kappa_3^{(22)}$ and $\kappa_3^{(33)} = \kappa_3^{(13)} = \kappa_3^{(23)} = 0$. In these cases Eqs. (84) reduce to

$$\begin{aligned} i \frac{\partial \psi_1}{\partial t} = & -\frac{\hbar}{4\mu} \nabla^2 \psi_1 + \chi_3 \psi_3 \psi_1^* + \bar{\kappa} |\psi_1|^2 \psi_1, \\ i \frac{\partial \psi_3}{\partial t} = & -\frac{\hbar}{2m_3} \nabla^2 \psi_3 + \Delta \omega \psi_3 + \chi_3 \psi_1^2, \end{aligned} \quad (85)$$

where we have defined $\bar{\kappa} \equiv \kappa_3 + (\kappa_3^{(11)} + \kappa_3^{(22)})/2$.

The coupled atomic/molecular soliton dynamics can be studied by direct numerical simulation of the above equations, starting with initial Gaussian atomic and molecular mean fields. The results of simulations are given in Figs. 2 and 3, where we plot the density profiles $|\psi_{1,2}|^2$ and $|\psi_3|^2$ as depending on time t and the radial coordinate $r = |\mathbf{x}|$. This demonstrates stable propagation of coupled atomic and molecular solitons, for two values of $\bar{\kappa}$ corresponding, respectively, to previously considered cases: (i) $\kappa_3^{(11)} = \kappa_3^{(22)} = 0$, so that $\bar{\kappa} = \kappa_3$, and (ii) $\kappa_3^{(11)} = \kappa_3^{(22)} = 2\kappa_3$, so that $\bar{\kappa} = 3\kappa_3$. The graphs represent a phase matched ($\Delta \omega = 0$) parametric inter-

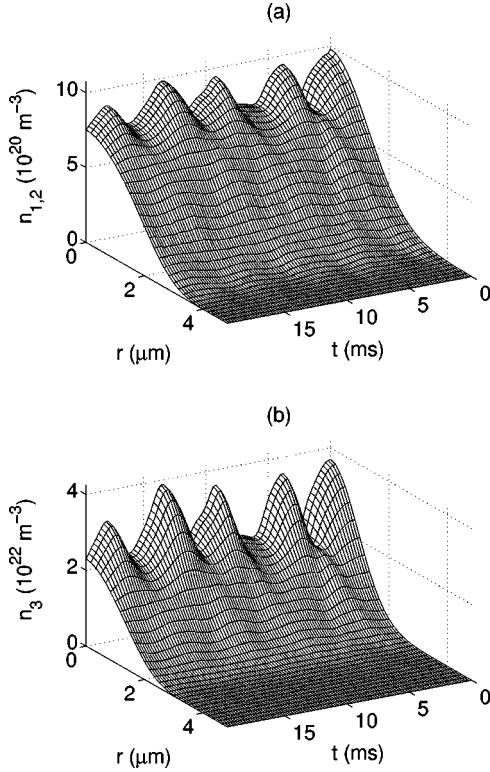


FIG. 3. Same as in Fig. 2 but for the value of $\bar{\kappa} = 19.8 \times 10^{-17} \text{ m}^3/\text{s}$ ($\kappa_3^{(11)}/2 = \kappa_3^{(22)}/2 = \kappa_3 = 6.6 \times 10^{-17} \text{ m}^3/\text{s}$). The initial optimum Gaussian parameters are $g_1 = g_2 \approx 3.13 \times 10^{10} \text{ m}^{-3/2}$, $g_3 \approx 1.92 \times 10^{10} \text{ m}^{-3/2}$, $w_1 = w_2 \approx 1.8 \text{ } \mu\text{m}$, and $w_3 \approx 1.3 \text{ } \mu\text{m}$.

action, with the initial optimum Gaussian parameters evaluated for $N = 10^6$. Clearly the Gaussian profile is only an approximate version of the true soliton envelope (which can be calculated numerically, as in [16]); hence we observe small in-phase oscillations. We note that although the case of Fig. 2 has higher energy than the low-density regime of a quantum gas of independent “dressed” molecules, nevertheless it appears from the mean-field theory that soliton propagation can be possible as a metastable regime, presumably with quantum evaporation.

This soliton propagation behavior leads to the remarkable property that coupled BEC solitons or localized matter-waves could be generated in three space dimensions without an external trapping potential. Similar spatiotemporal solitons have recently been observed with optical fields, but in the degenerate case of parametric interaction [40]. The results of the present nondegenerate theory indicate that additional s -wave scatterings (or phase modulation processes, in the optical case) that exist among all three fields would tend to make solitons less stable than in the degenerate case.

C. “Superchemistry” behavior

Another possible experimental approach to generating the coupled condensates is by first cooling an atomic vapor to a BEC, and then switching on the atom-molecule coupling. This can lead to the formation of the molecular condensate

and a “superchemistry” dynamics, where the condensate interconversion is dominated by the coherent stimulated emission of bosonic atoms or molecules into their respective condensates. The phenomenon would be the matter-wave analog to optical frequency summation.

We note that similar behavior, in the case of degenerate parametric interaction, has recently been studied for a Feshbach resonance coupling of single atomic and molecular condensates [41]. Assuming uniform condensate wave functions, the system was analyzed in the context of quantum tunneling emerging from the oscillatory behavior of the number of atoms and molecules in their respective condensates. The oscillatory dynamics was in response to a sudden change of the detuning of the resonance, applied to a homogeneous atomic/molecular BEC that was initially in equilibrium.

For the case of Raman photoassociation coupling, and a trapped atomic BEC as the initial condition, the nonlinear dynamics of the coupled condensates was studied in [22] by direct simulation of the resulting degenerate MFT equations. This gave further insights into the rich variety of dynamical behavior and a theoretical prediction of the possibility of coherent chemistry or “superchemistry” behavior in coupled BEC systems.

Here we extend this study to the case of two atomic and one molecular condensates, and analyze the nondegenerate MFT equations modified by the trap potential terms. The trap terms are of the form $V_i(\mathbf{x})\psi_i$ ($i = 1, 2, 3$), to be added on the right-hand sides of Eqs. (84). We consider a rotationally symmetric harmonic trap potential $V_i(\mathbf{x}) = m_i \omega_i^2 |\mathbf{x}|^2 / (2\hbar)$, where ω_i is the trap oscillation frequency for the i th species, and restrict our analysis to the symmetric case of $\psi_1(\mathbf{x}) = \psi_2(\mathbf{x})$, with $\kappa_3^{(11)} = \kappa_3^{(22)} = 2\kappa_3$ and $\kappa_3^{(33)} = \kappa_3^{(13)} = \kappa_3^{(23)} = 0$. In addition, we choose $\Delta\omega = 1.5 \times 10^4 \text{ s}^{-1}$ and the trap frequencies $\omega_1/2\pi = \omega_2/2\pi = \omega_3/2\pi = 100 \text{ Hz}$.

We simulate Eqs. (85) together with the trap potential terms in two stages. In the first stage, we assume that the parametric coupling χ_3 is switched off, and that only atomic species are present in the trap. The result achieved is the steady state of the Gross-Pitaevskii equations for a two-component atomic Bose condensate, which we choose to correspond to an initial total number of atomic particles $N = \bar{N}_1 + \bar{N}_2 \sim 4.8 \times 10^4$ at a concentration of $n \sim 5 \times 10^{19} \text{ m}^{-3}$. This provides the starting condition for the second stage of simulations, where we switch on the coupling χ_3 . The results are shown in Fig. 4, where we observe giant collective oscillations between the atomic and molecular condensates, which take place on short time scales. These oscillations are due to the coherent process of stimulated emission into a condensate of molecular dimers, followed by the reverse process of stimulated emission into the atomic condensates. The integrated number of particles in the atomic and molecular condensates as depending on time is shown in Fig. 5.

This “superchemistry” is a type of coherent chemical reaction that can take place in BEC systems at ultralow temperatures. It is characterized by Bose-enhanced reaction rates ($\dot{n}_{j(3)} \propto n_j \sqrt{n_3}$, $j = 1, 2$) due to the effect of bosonic stimulated emission. This is in a sharp contrast to the predictions

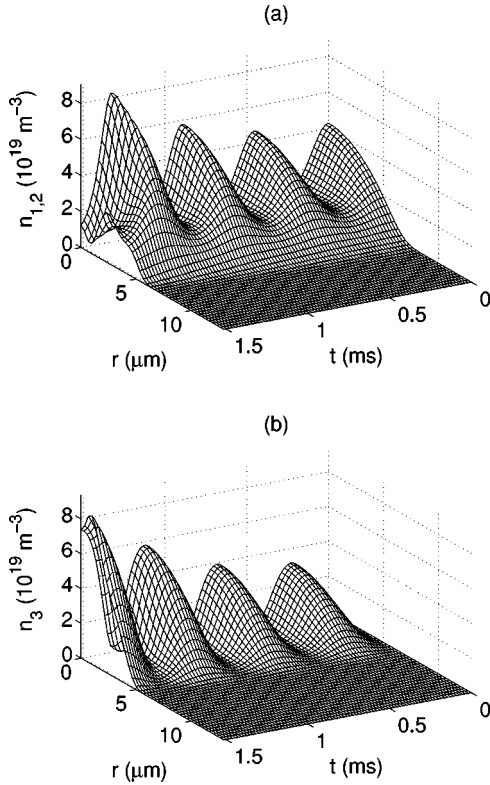


FIG. 4. “Superchemistry” oscillations: atomic (a) and molecular (b) condensate densities $n_i = |\phi_i(\mathbf{x}, t)|^2$ as depending on time t and the radial distance $r = |\mathbf{x}|$ from the trap center. The values of parameters are $\bar{\kappa} = 19.8 \times 10^{-17} \text{ m}^3/\text{s}$ ($\kappa_3^{(11)}/2 = \kappa_3^{(22)}/2 = \kappa_3 = 6.6 \times 10^{-17} \text{ m}^3/\text{s}$), $\kappa_3^{(33)} = \kappa_3^{(13)} = \kappa_3^{(23)} = 0$, $m_1 = m_2 = 10^{-25} \text{ kg}$, $\chi_3 = 10^{-6} \text{ m}^3/\text{s}$, $\Delta\omega = 1.5 \times 10^4 \text{ s}^{-1}$, and $\omega_1/2\pi = \omega_2/2\pi = \omega_3/2\pi = 100 \text{ Hz}$.

of conventional (Boltzmann) chemical kinetics, where the chemical reaction rates do not depend on the number of product particles and go to zero at low temperatures, according to the Arrhenius law. We emphasize that this type of coherent density dependent oscillation is a signature of the nonlinear parametric coupling, and would represent a first step toward observing the liquid-gas phase transition discussed earlier.

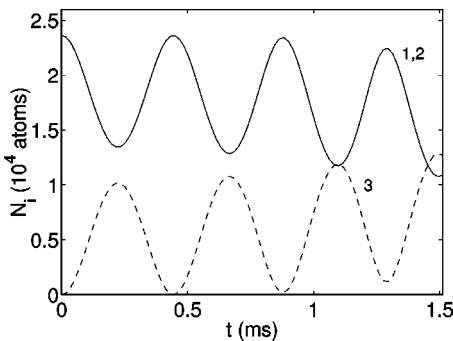


FIG. 5. Total number of particles in the atomic (1,2) and molecular (3) Bose condensates $\bar{N}_i = \int d^3\mathbf{x} |\phi_i(\mathbf{x}, t)|^2$ as a function of time t .

VII. SUMMARY

In summary, we have presented quantum soliton or bound-state solutions to a nondegenerate parametric quantum field theory, in one, two, and three space dimensions. As in the degenerate parametric case, the results have quantum pointlike (zero-radius) structures in the eigenstates in more than one space dimension, if there is no momentum cutoff. This is quite different from the behavior of solitons in the corresponding classical theory, and the reason for this is the inherently nonclassical structure of the bound state, which is a quantum superposition state. We note that most previous analyses of quantum solitons treated cases where the quantum soliton was at least qualitatively similar to the corresponding classical theory. This is not the case here.

With the inclusion of momentum cutoffs on the nonlinear couplings, the two-particle bound state has a finite radius, even in the simplest case of a pure parametric interaction—i.e., without the quartic interaction term. We can estimate, in the case of nonlinear optical or atomic BEC interactions, that the nonlinear couplings should have a momentum cutoff no higher than an inverse carrier wavelength or inverse scattering length, respectively. These estimates can be improved by more careful treatment of the theory at large relative momenta. Such an improved treatment would be especially appropriate in the three-dimensional case where we obtain a linear divergence with $k_m \rightarrow \infty$.

Most significantly, the quantum solitons form in physically testable regimes. Our estimates for characteristic soliton radii and binding energies, in the case of photonic interactions in highly nonlinear parametric ($\chi^{(2)}$) media, result in much more realistic values than examples of $\chi^{(3)}$ solitons, with the required experimental environment being nearly available with current technology. In the case of BEC interactions, we point out the possibility of transition between the quantum (diboson) soliton regime, where atoms couple to form molecules in a local way, to a classical soliton regime. In the classical domain, the coherent coupling of three entire condensates takes the place of the nonlinear optical process of sum-frequency generation. This gives the possibility of simultaneous atom and molecular matter-wave solitons in three space dimensions, and therefore an intense, stable, and nondiverging atom/molecular laser output. The stability properties of these solitons depend on the details of the s -wave scattering lengths between all three species present. We note that earlier examples of matter-wave BEC type solitons (see, e.g., [42], and references therein) were only for a one dimensional geometry. Of even more interest is a type of coherent BEC-enhanced chemical reaction or “superchemistry” behavior at ultralow temperatures, which follows from the underlying dynamics of coupled condensate nonlinear equations.

Finally, the bosonic character of the fields is not relevant for the quantum bound-state theory derived here. Exactly the same results would occur if fermionic fields were involved, and we changed the corresponding commutation relations to anticommutators. In this respect, the present theory differs from the degenerate case [11,23], where the results were only applicable to bosonic fields. This suggests that part of

these results (but not the classical soliton theory) could be extended to possible atomic fermionic superconductors, in which coupling between fermionic atoms is enhanced by the coherent production of bosonic molecules. Another possible application is to models of mesonlike coupling in mixed fermionic-bosonic systems.

ACKNOWLEDGMENTS

We acknowledge the Australian Research Council for the support of this work, and are grateful to D. Heinzen for stimulating discussions.

APPENDIX A

To calculate the energy

$$\tilde{E}_0^{(N)} = \langle \tilde{\varphi}_0^{(N)} | \hat{H} | \tilde{\varphi}_0^{(N)} \rangle / \langle \tilde{\varphi}_0^{(N)} | \tilde{\varphi}_0^{(N)} \rangle$$

with the ansatz (44) we first transform to the coordinates $\mathbf{x} = \mathbf{R} + m_2 \mathbf{r}/M$ and $\mathbf{y} = \mathbf{R} - m_1 \mathbf{r}/M$, and use binomial expansion, so that $|\tilde{\varphi}_0^{(N)}\rangle$ becomes

$$\begin{aligned} |\tilde{\varphi}_0^{(N)}\rangle &= \left(\int d^D \mathbf{x} \hat{\Psi}_3^\dagger(\mathbf{x}) + \int \int d^D \mathbf{x} d^D \mathbf{y} \right. \\ &\quad \times g(\mathbf{x} - \mathbf{y}) \hat{\Psi}_1^\dagger(\mathbf{x}) \hat{\Psi}_2^\dagger(\mathbf{y}) \Big)^{N/2} |0\rangle \\ &= \sum_{j=0}^{N/2} \binom{N/2}{j} \left(\int d^D \mathbf{x} \hat{\Psi}_3^\dagger(\mathbf{x}) \right)^{N/2-j} \left(\int \int d^D \mathbf{x} d^D \mathbf{y} \right. \\ &\quad \times g(\mathbf{x} - \mathbf{y}) \hat{\Psi}_1^\dagger(\mathbf{x}) \hat{\Psi}_2^\dagger(\mathbf{y}) \Big)^j |0\rangle. \end{aligned}$$

Here the vacuum state $|0\rangle$ is defined as $|0\rangle = |0_1\rangle|0_2\rangle|0_3\rangle$, so that $\hat{\Psi}_i|0_i\rangle = 0$.

Calculating the averages involved in $\tilde{E}_0^{(N)}$ uses the commutation relations $[\hat{\Psi}_i(\mathbf{x}), \hat{\Psi}_j^\dagger(\mathbf{x}')] = \delta_{ij} \delta(\mathbf{x} - \mathbf{x}')$, and relies on the zero-radius property of the two-particle correlation function $g(\mathbf{r})$, i.e. $g(\mathbf{r}) = 0$ for $\mathbf{r} \neq 0$ and $g(0) = -\chi_D/\kappa_D$, in two and three dimensions. We demonstrate this on the example of $\langle \tilde{\varphi}_0^{(N)} | \tilde{\varphi}_0^{(N)} \rangle$ which is written using the above expansion as

$$\begin{aligned} \langle \tilde{\varphi}_0^{(N)} | \tilde{\varphi}_0^{(N)} \rangle &= \sum_{j'=0}^{N/2} \sum_{j=0}^{N/2} \binom{N/2}{j'} \\ &\quad \times \binom{N/2}{j} \langle 0_3 | \left(\int d^D \mathbf{x}' \hat{\Psi}_3(\mathbf{x}') \right)^{N/2-j'} \\ &\quad \times \left(\int d^D \mathbf{x} \hat{\Psi}_3^\dagger(\mathbf{x}) \right)^{N/2-j} |0_3\rangle \\ &\quad \times \langle 0_1, 0_2 | \left(\int \int d^D \mathbf{x}' d^D \mathbf{y}' g(\mathbf{x}' - \mathbf{y}') \right. \\ &\quad \times \hat{\Psi}_1(\mathbf{x}') \hat{\Psi}_2(\mathbf{y}') \Big)^{j'} \left(\int \int d^D \mathbf{x} d^D \mathbf{y} \right. \\ &\quad \times g(\mathbf{x} - \mathbf{y}) \hat{\Psi}_1^\dagger(\mathbf{x}) \hat{\Psi}_2^\dagger(\mathbf{y}) \Big)^j |0_1, 0_2\rangle. \end{aligned}$$

We first simplify the calculation by applying the commutation relations and reordering the operators so that all destruction operators stand on the right. Then all terms with $j \neq j'$ in the above double sum will vanish due to extra factors $\hat{\Psi}_i(\mathbf{x})$ [or $\hat{\Psi}_i^\dagger(\mathbf{x})$] acting on the vacuum state $|0_i\rangle$ from the right (or on $\langle 0_i|$ from the left). The remaining terms with $j' = j$ are combined into a single sum according to

$$\sum_{j'=0}^{N/2} \sum_{j=0}^{N/2} \{ \dots \}_{j',j} = \sum_{j'=0}^{N/2} \sum_{j=0}^{N/2} \{ \dots \}_{j',j} \delta_{j',j} = \sum_{j=0}^{N/2} \{ \dots \}_{j'=j}.$$

The nonvanishing terms in this sum contain no operators and can be further simplified by integrating with respect to δ functions from the commutators. The result of these integrations is that all terms, except the one corresponding to $j = 0$, will contain factors of the form $\int \int d^D \mathbf{x} d^D \mathbf{y} g^2(\mathbf{x} - \mathbf{y})$ which vanish due to the zero-radius property of the $g(\mathbf{r})$ function [$\int d^D \mathbf{r} g^2(\mathbf{r}) = 0$] in two and three dimensions ($D = 2, 3$). The remaining nonvanishing contribution of the term with $j = 0$ results in

$$\begin{aligned} \langle \tilde{\varphi}_0^{(N)} | \tilde{\varphi}_0^{(N)} \rangle &= \langle 0_3 | \left(\int d^D \mathbf{x}' \hat{\Psi}_3(\mathbf{x}') \right)^{N/2} \left(\int d^D \mathbf{x} \hat{\Psi}_3^\dagger(\mathbf{x}) \right)^{N/2} |0_3\rangle \\ &= (N/2)! \left(\int d^D \mathbf{x} \right)^{N/2} = (N/2)! V^{N/2} \quad (D=2,3), \end{aligned}$$

where $V \equiv \int d^D \mathbf{x}$.

Similar calculations apply to the other averages involved in $\langle \tilde{\varphi}_0^{(N)} | \hat{H} | \tilde{\varphi}_0^{(N)} \rangle$, so that one can obtain (for $D = 2, 3$)

$$\begin{aligned} \langle \tilde{\varphi}_0^{(N)} | \hat{H} | \tilde{\varphi}_0^{(N)} \rangle &= (N/2)! V^{N/2} \frac{N}{2} \left[\frac{\hbar^2}{2\mu} \int d^D \mathbf{x} |\nabla g(\mathbf{x})|^2 \right. \\ &\quad + \hbar \Delta \omega + 2\hbar \chi_D g(0) + \hbar \kappa_D g^2(0) \\ &\quad \left. + \left(\frac{N}{2} - 1 \right) \frac{\hbar \kappa_D^{(33)}}{2V} \right]. \end{aligned}$$

Here the contribution from the kinetic energy part $\int d^D \mathbf{x} |\nabla g(\mathbf{x})|^2 = -\int d^D \mathbf{x} g(\mathbf{x}) \nabla^2 g(\mathbf{x})$ can be shown to vanish, using Eq. (15) and the property that $\int d^D \mathbf{x} g^2(\mathbf{x}) = 0$ ($D = 2, 3$). Substituting then $g(0) = -\chi_D/\kappa_D$ from Eq. (35) we finally obtain

$$\begin{aligned} \tilde{E}_0^{(N)} &= \frac{N}{2} \left(\hbar \Delta \omega - \frac{\hbar (\chi_D)^2}{\kappa_D} \right) + \frac{N}{4} \left(\frac{N}{2} - 1 \right) \frac{\hbar \kappa_D^{(33)}}{V} \\ &\quad (D=2,3), \end{aligned}$$

which is the result given in Eq. (45).

For the case of odd values of N the N -particle ansatz contains an extra factor of $\int d^D \mathbf{x} \hat{\Psi}_3^\dagger(\mathbf{x})$ acting on the vacuum state $|0\rangle$ from the left, in Eq. (44), and $N/2$ is replaced by its integer part $[N/2]$. The final result for the energy $\tilde{E}_0^{(N)}$ in this case has the form of the above equation where the same replacement $N/2 \rightarrow [N/2]$ is applied.

APPENDIX B

To calculate the N -particle energy $\tilde{E}_0^{(N)}(k_m)$ $= \langle \tilde{\varphi}_0^{(N)}(k_m) | \hat{H} | \tilde{\varphi}_0^{(N)}(k_m) \rangle / \langle \tilde{\varphi}_0^{(N)}(k_m) | \tilde{\varphi}_0^{(N)}(k_m) \rangle$ with the cutoff dependent ansatz (64) and the Hamiltonian given by Eqs. (1), (50), and (51), we first use the binomial expansion, so that

$$\begin{aligned} |\tilde{\varphi}_0^{(N)}(k_m)\rangle &= \left(\hat{a}_3^\dagger(0) + (2\pi)^{-D/2} \right. \\ &\quad \times \left. \int_{|\mathbf{k}|=0}^{k_m} d^D \mathbf{k} G(\mathbf{k}) \hat{a}_1^\dagger(\mathbf{k}) \hat{a}_2^\dagger(-\mathbf{k}) \right)^{N/2} |0\rangle \\ &= \sum_{j=0}^{N/2} \binom{N/2}{j} [\hat{a}_3^\dagger(0)]^{N/2-j} \left((2\pi)^{-D/2} \right. \\ &\quad \times \left. \int_{|\mathbf{k}|=0}^{k_m} d^D \mathbf{k} G(\mathbf{k}) \hat{a}_1^\dagger(\mathbf{k}) \hat{a}_2^\dagger(-\mathbf{k}) \right)^j |0\rangle, \end{aligned}$$

where we assume N is even, and the vacuum state $|0\rangle = |0_1\rangle|0_2\rangle|0_3\rangle$ is defined such that $\hat{a}_i|0_i\rangle = 0$.

We show the main steps involved in the calculation of $\tilde{E}_0^{(N)}(k_m)$ on the example of $\langle \tilde{\varphi}_0^{(N)}(k_m) | \tilde{\varphi}_0^{(N)}(k_m) \rangle$. Using the above expansion, $\langle \tilde{\varphi}_0^{(N)}(k_m) | \tilde{\varphi}_0^{(N)}(k_m) \rangle$ is expressed as a double sum $\sum_{j'=0}^{N/2} \sum_{j=0}^{N/2} \{ \dots \}_{j',j}$, which is reduced to a single sum $\sum_{j=0}^{N/2} \{ \dots \}_{j,j'}$ as the terms with $j' \neq j$ will vanish, after reordering the operators, due to the unequal number of creation and destruction operators acting on the vacuum. The terms that can give nonvanishing contributions are written as

$$\begin{aligned} \langle \tilde{\varphi}_0^{(N)}(k_m) | \tilde{\varphi}_0^{(N)}(k_m) \rangle &= \sum_{j=0}^{N/2} \binom{N/2}{j}^2 \langle 0_3 | [\hat{a}_3(0)]^{N/2-j} [\hat{a}_3^\dagger(0)]^{N/2-j} | 0_3 \rangle \\ &\quad \times \langle 0_1, 0_2 | \\ &\quad \times \left((2\pi)^{-D/2} \int_{|\mathbf{k}'|=0}^{k_m} d^D \mathbf{k}' G(\mathbf{k}') \hat{a}_1(\mathbf{k}') \hat{a}_2(-\mathbf{k}') \right)^j \\ &\quad \times \left((2\pi)^{-D/2} \int_{|\mathbf{k}|=0}^{k_m} d^D \mathbf{k} G(\mathbf{k}) \hat{a}_1^\dagger(\mathbf{k}) \hat{a}_2^\dagger(-\mathbf{k}) \right)^j | 0_1, 0_2 \rangle. \end{aligned} \quad (\text{B1})$$

Here the calculation of the averages $\langle 0_3 | \dots | 0_3 \rangle$ and $\langle 0_1, 0_2 | \dots | 0_1, 0_2 \rangle$ uses the commutation relations $[\hat{a}_i(\mathbf{k}), \hat{a}_j^\dagger(\mathbf{k}')] = \delta_{ij} \delta(\mathbf{k} - \mathbf{k}')$ to change the order of creation and destruction operators in the operator products, so that all the destruction operators act on the vacuum from the right, while the creation operators act on the vacuum from the left. This gives vanishing terms and simultaneously generates nonvanishing terms due to the δ functions from the commutators. For the case of the average $\langle 0_3 | \dots | 0_3 \rangle$ the nonvanishing terms give

$$\langle 0_3 | [\hat{a}_3(0)]^{N/2-j} [\hat{a}_3^\dagger(0)]^{N/2-j} | 0_3 \rangle = \left(\frac{N}{2} - j \right)! \delta(0)^{N/2-j}, \quad (\text{B2})$$

where $\delta(0)$ is to be understood as $\delta(0) = \int d^D \mathbf{x} / (2\pi) = V / (2\pi)$ in the limit of infinitely large volume $V \rightarrow \infty$.

Similarly, reordering the operators in $\langle 0_1, 0_2 | \dots | 0_1, 0_2 \rangle$ produces nonvanishing terms involving products of δ functions, so that

$$\begin{aligned} \langle 0_1, 0_2 | &\left((2\pi)^{-D/2} \int_{|\mathbf{k}'|=0}^{k_m} d^D \mathbf{k}' G(\mathbf{k}') \hat{a}_1(\mathbf{k}') \hat{a}_2(-\mathbf{k}') \right)^j \\ &\times \left((2\pi)^{-D/2} \int_{|\mathbf{k}|=0}^{k_m} d^D \mathbf{k} G(\mathbf{k}) \hat{a}_1^\dagger(\mathbf{k}) \hat{a}_2^\dagger(-\mathbf{k}) \right)^j | 0_1, 0_2 \rangle \\ &= \prod_{p=1}^j \left(\frac{1}{(2\pi)^D} \int_{|\mathbf{k}'|=0}^{k_m} \int_{|\mathbf{k}_p|=0}^{k_m} d^D \mathbf{k}'_p d^D \mathbf{k}_p G(\mathbf{k}'_p) G(\mathbf{k}_p) \right) \\ &\quad \times \sum_{perm} [\delta(\mathbf{k}_{(1)} - \mathbf{k}'_1) \delta(\mathbf{k}_{(2)} - \mathbf{k}'_2) \dots \delta(\mathbf{k}_{(j)} - \mathbf{k}'_j)] \\ &\quad \times \sum_{perm} [\delta(\mathbf{k}_{(1)} - \mathbf{k}'_1) \delta(\mathbf{k}_{(2)} - \mathbf{k}'_2) \dots \delta(\mathbf{k}_{(j)} - \mathbf{k}'_j)], \end{aligned} \quad (\text{B3})$$

where \sum_{perm} represents summation with respect to permutations referring to the set of bracketed indices $[(1), (2), \dots, (j)]$ in the product of δ functions $\delta(\mathbf{k}_{(1)} - \mathbf{k}'_1) \delta(\mathbf{k}_{(2)} - \mathbf{k}'_2) \dots \delta(\mathbf{k}_{(j)} - \mathbf{k}'_j)$. There are $j!$ terms in each of the sums, such as

$$\begin{aligned} &\delta(\mathbf{k}_1 - \mathbf{k}'_1) \delta(\mathbf{k}_2 - \mathbf{k}'_2) \dots \delta(\mathbf{k}_j - \mathbf{k}'_j) + \delta(\mathbf{k}_2 - \mathbf{k}'_1) \\ &\quad \times \delta(\mathbf{k}_1 - \mathbf{k}'_2) \dots \delta(\mathbf{k}_j - \mathbf{k}'_j) + \dots \end{aligned}$$

The product of the two sums will contain diagonal terms, i.e., terms in which the permutation arrangement of the bracketed indices $[(1), (2), \dots, (j)]$ is the same in both sets of δ function products, so that these terms have the following form:

$$\begin{aligned} &\delta^2(\mathbf{k}_1 - \mathbf{k}'_1) \delta^2(\mathbf{k}_2 - \mathbf{k}'_2) \dots \delta^2(\mathbf{k}_j - \mathbf{k}'_j) \\ &\quad + \delta^2(\mathbf{k}_2 - \mathbf{k}'_1) \delta^2(\mathbf{k}_1 - \mathbf{k}'_2) \dots \delta^2(\mathbf{k}_j - \mathbf{k}'_j) + \dots \end{aligned}$$

The remaining terms are the off-diagonal terms in which the arrangement of indices is different, as in a term like

$$\begin{aligned} &\delta(\mathbf{k}_1 - \mathbf{k}'_1) \delta(\mathbf{k}_2 - \mathbf{k}'_2) \delta(\mathbf{k}_3 - \mathbf{k}'_3) \dots \delta(\mathbf{k}_j - \mathbf{k}'_j) \\ &\quad \times \delta(\mathbf{k}_2 - \mathbf{k}'_1) \delta(\mathbf{k}_1 - \mathbf{k}'_2) \delta(\mathbf{k}_3 - \mathbf{k}'_3) \dots \delta(\mathbf{k}_j - \mathbf{k}'_j). \end{aligned}$$

The diagonal terms can be combined into a single sum over the number of permutations with respect to the set of bracketed indices:

$$\sum_{perm} [\delta^2(\mathbf{k}_{(1)} - \mathbf{k}'_1) \delta^2(\mathbf{k}_{(2)} - \mathbf{k}'_2) \dots \delta^2(\mathbf{k}_{(j)} - \mathbf{k}'_j)].$$

The integrations in Eq. (B3) over the δ functions involved in these diagonal terms will result in a factor of $j! \delta(0)^j$. The integrations over the δ functions in the off-diagonal terms can produce a factor of $\delta(0)^k$ only with $k < j$, and therefore the contribution of these terms can be neglected as compared to the contribution of the diagonal terms in the limit of $V \rightarrow \infty$. This results in

$$\begin{aligned} & \prod_{p=1}^j \left(\frac{1}{(2\pi)^D} \int_{|\mathbf{k}'_p|=0}^{k_m} \int_{|\mathbf{k}_p|=0}^{k_m} d^D \mathbf{k}'_p d^D \mathbf{k}_p G(\mathbf{k}'_p) G(\mathbf{k}_p) \right) \\ & \times \left(\sum_{perm} [\delta^2(\mathbf{k}_{(1)} - \mathbf{k}'_1) \delta^2(\mathbf{k}_{(2)} - \mathbf{k}'_2) \cdots \delta^2(\mathbf{k}_{(j)} - \mathbf{k}'_j)] \right) \\ & = j! \delta(0)^j \left(\frac{1}{(2\pi)^D} \int_{|\mathbf{k}|=0}^{k_m} d^D \mathbf{k}_p G^2(\mathbf{k}_p) \right)^j. \end{aligned} \quad (\text{B4})$$

Combining Eqs. (B1)–(B4) we obtain

$$\begin{aligned} & \langle \tilde{\varphi}_0^{(N)}(k_m) | \tilde{\varphi}_0^{(N)}(k_m) \rangle \\ & = (N/2)! \delta(0)^{N/2} \sum_{j=0}^{N/2} \binom{N/2}{j} \left(\frac{1}{(2\pi)^D} \int_{|\mathbf{k}|=0}^{k_m} d^D \mathbf{k} G^2(\mathbf{k}) \right)^j \\ & = (N/2)! \delta(0)^{N/2} \left(1 + \frac{1}{(2\pi)^D} \int_{|\mathbf{k}|=0}^{k_m} d^D \mathbf{k}_p G^2(\mathbf{k}_p) \right)^{N/2}. \end{aligned}$$

Applying similar procedures to other averages involved in $\langle \tilde{\varphi}_0^{(N)}(k_m) | \hat{H} | \tilde{\varphi}_0^{(N)}(k_m) \rangle$ and keeping only the leading terms $\sim \delta(0)^{N/2}$ we obtain that

$$\begin{aligned} \tilde{E}_0^{(N)}(k_m) & = \frac{\langle \tilde{\varphi}_0^{(N)}(k_m) | \hat{H} | \tilde{\varphi}_0^{(N)}(k_m) \rangle}{\langle \tilde{\varphi}_0^{(N)}(k_m) | \tilde{\varphi}_0^{(N)}(k_m) \rangle} \\ & = \frac{N}{2} [1 + F(r_0, k_m)]^{-1} \left(\frac{\hbar^2}{2\mu} R(r_0, k_m) + \hbar \Delta \omega \right. \\ & \quad \left. + 2\hbar \chi_D g(0, k_m) + \hbar \kappa_D g^2(0, k_m) \right), \end{aligned}$$

where we have defined

$$F(r_0, k_m) \equiv \frac{1}{(2\pi)^D} \int_{|\mathbf{k}|=0}^{k_m} d^D \mathbf{k} G^2(\mathbf{k}),$$

$$R(r_0, k_m) \equiv \frac{1}{(2\pi)^D} \int_{|\mathbf{k}|=0}^{k_m} d^D \mathbf{k} k^2 G^2(\mathbf{k}),$$

and

$$g(0, k_m) = \frac{1}{(2\pi)^D} \int_{|\mathbf{k}|=0}^{k_m} d^D \mathbf{k} G(\mathbf{k}).$$

We next note that for the case $N=2$ the expression for $\tilde{E}_0^{(N)}(k_m)$ must give the exact two-particle solution for the energy $E_0^{(2)}(k_m)$, given by Eqs. (54) and (62), i.e.,

$$\tilde{E}_0^{(2)}(k_m) = E_0^{(2)}(k_m) = -\hbar^2/(2\mu r_0^2),$$

and therefore

$$\begin{aligned} & [1 + F(r_0, k_m)]^{-1} \left(\frac{\hbar^2}{2\mu} R(r_0, k_m) + \hbar \Delta \omega + 2\hbar \chi_D g(0, k_m) \right. \\ & \quad \left. + \hbar \kappa_D g^2(0, k_m) \right) = -\hbar^2/(2\mu r_0^2). \end{aligned} \quad (\text{B5})$$

Thus our final step in proving Eq. (65) consists in showing that Eq. (B5) is equivalent to the eigenvalue equation (62). This equivalence can be shown with the use of the explicit expression for $G(\mathbf{k})$, from Eq. (53),

$$G(\mathbf{k}) = -\frac{q}{k^2 + 1/r_0^2},$$

which allows one to express $R(r_0, k_m)$ as

$$R(r_0, k_m) = \frac{q^2}{r_0^{D-2}} f_D(r_0 k_m) - \frac{1}{r_0^2} F(r_0, k_m).$$

In addition, we use the definition of q , Eq. (56), and express $g(0, k_m)$ in terms of $f_D(r_0 k_m)$, using Eq. (57). This makes it possible to rewrite Eq. (B5) in the form of Eq. (62), thus proving that $\tilde{E}_0^{(2)}(k_m) = E_0^{(2)}(k_m)$, and therefore

$$\tilde{E}_0^{(N)}(k_m) = \frac{N}{2} E_0^{(2)}(k_m),$$

which is the result of Eq. (65).

- [1] N.H. Christ and T.D. Lee, Phys. Rev. D **12**, 1606 (1975); T. D. Lee, *Particle Physics and Introduction to Field Theory* (Harwood, Switzerland, 1988).
- [2] E.H. Lieb and W. Liniger, Phys. Rev. **130**, 1605 (1963); I.B. McGuire, J. Math. Phys. **5**, 622 (1964); C.N. Yang, Phys. Rev. **168**, 1920 (1967); H.B. Thacker, Rev. Mod. Phys. **53**, 253 (1981).
- [3] S.J. Carter, P.D. Drummond, M.D. Reid, and R.M. Shelby, Phys. Rev. Lett. **58**, 1841 (1987); P.D. Drummond and S.J. Carter, J. Opt. Soc. Am. B **4**, 1565 (1987).

- [4] Y. Lai and H.A. Haus, Phys. Rev. A **40**, 844 (1989); H.A. Haus and Y. Lai, J. Opt. Soc. Am. B **7**, 386 (1990).
- [5] M. Rosenbluh and R.M. Shelby, Phys. Rev. Lett. **66**, 153 (1991); P.D. Drummond, R.M. Shelby, S.R. Friberg, and Y. Yamamoto, Nature (London) **365**, 307 (1993).
- [6] C.L. Schultz, M.J. Ablowitz, and O. BarYaacov, Phys. Rev. Lett. **59**, 2825 (1987); G.D. Pang, F.-C. Pu, and B.-H. Zhao, *ibid.* **65**, 3227 (1990); G.D. Pang, Phys. Lett. A **184**, 163 (1994).
- [7] R.B. Laughlin, Phys. Rev. Lett. **50**, 1385 (1983).

- [8] D.C. Tsui, H.L. Störmer, and H.C. Gossard, *Phys. Rev. Lett.* **48**, 1559 (1982).
- [9] N.K. Wilkin, J.M.F. Gunn, and R.A. Smith, *Phys. Rev. Lett.* **80**, 2265 (1998).
- [10] M.H. Anderson, J.R. Ensher, C.E. Wieman and E.A. Cornell, *Science* **269**, 198 (1995); C.C. Bradley, C.A. Sackett, J.J. Tollett, and R.G. Hulet, *Phys. Rev. Lett.* **75**, 1687 (1995); K.B. Davis, M.O. Mewes, M.R. Andrews, N.J. van Druten, D.S. Durfee, D.M. Kurn, and W. Ketterle, *ibid.* **75**, 3969 (1995).
- [11] K.V. Kheruntsyan and P.D. Drummond, *Phys. Rev. A* **58**, 2488 (1998).
- [12] R. Friedberg and T.D. Lee, *Phys. Rev. B* **40**, 6745 (1989).
- [13] Y. Wang, *Phys. Lett. A* **176**, 19 (1993).
- [14] P.D. Drummond and H. He, *Phys. Rev. A* **56**, R1107 (1997).
- [15] A.A. Kanashov and A.M. Rubenchik, *Physica D* **4**, 122 (1981).
- [16] K. Hayata and M. Koshiba, *Phys. Rev. Lett.* **71**, 3275 (1993); L. Torner, C.R. Menyuk, W.E. Torruellas, and G.I. Stegeman, *Opt. Lett.* **20**, 13 (1995); L. Bergé, V.K. Mezentsev, J.J. Rasmussen, and J. Wyller, *Phys. Rev. A* **52**, R28 (1995); H. He, M.J. Werner, and P.D. Drummond, *Phys. Rev. E* **54**, 896 (1996); A.V. Buryak and Yu. Kivshar, *Phys. Rev. Lett.* **77**, 5210 (1996).
- [17] B.A. Malomed, P.D. Drummond, H. He, A. Berntson, D. Anderson, and M. Lisak, *Phys. Rev. E* **56**, 4725 (1997).
- [18] W.E. Torruellas, Z. Wang, D.J. Hagan, E.W. Van Stryland, G.I. Stegeman, L. Torner, and C.R. Menyuk, *Phys. Rev. Lett.* **74**, 5036 (1995); R. Schiek, Y. Baek, and G.I. Stegeman, *Phys. Rev. E* **53**, 1138 (1996).
- [19] K.V. Kheruntsyan and P.D. Drummond, *Phys. Rev. A* **58**, R2676 (1998).
- [20] P.D. Drummond, K.V. Kheruntsyan, and H. He, *J. Opt. B: Quantum Semiclass. Opt.* **1**, 387 (1999).
- [21] I.H. Deutsch and R.Y. Chiao, *Phys. Rev. Lett.* **69**, 3627 (1992); Z. Cheng and G. Kurizki, *ibid.* **75**, 3430 (1995); I.H. Deutsch, R.Y. Chiao, and J.C. Garrison, *Phys. Rev. A* **47**, 3330 (1993); A.G. Shnirman, B.A. Malomed, and E. Ben-Jacob, *ibid.* **50**, 3453 (1994).
- [22] D.J. Heinzen, R.H. Wynar, P.D. Drummond, and K.V. Kheruntsyan, *Phys. Rev. Lett.* (to be published); see also D.J. Heinzen, P.D. Drummond, and K.V. Kheruntsyan, *Bull. Am. Phys. Soc.* **44**(1), 1007 (1999).
- [23] P.D. Drummond, K.V. Kheruntsyan, and H. He, *Phys. Rev. Lett.* **81**, 3055 (1998).
- [24] C.J. Myatt *et al.*, *Phys. Rev. Lett.* **78**, 586 (1997); H. Pu and N.P. Bigelow, *ibid.* **80**, 1130 (1998); C.K. Law *et al.*, *ibid.* **79**, 3105 (1997); B.D. Esry *et al.*, *ibid.* **78**, 3594 (1997) P. Öhberg, *Phys. Rev. A* **59**, 634 (1999).
- [25] A.V. Buryak, Yu.S. Kivshar, and S. Trillo, *Opt. Lett.* **20**, 1961 (1995); M.A. Karpierz, *ibid.* **20**, 1677 (1995); S. Trillo, A.V. Buryak, and Yu.S. Kivshar, *Opt. Commun.* **122**, 200 (1996); O. Bang, *J. Opt. Soc. Am. B* **14**, 51 (1997); L. Bergé, O. Bang, J.J. Rasmussen, and V.K. Mezentsev, *Phys. Rev. E* **55**, 3555 (1997); O. Bang, Yu.S. Kivshar, A.V. Buryak, A. De Rossi, and S. Trillo, *ibid.* **58**, 5057 (1998).
- [26] T.D. Lee, *Phys. Rev.* **54**, 1329 (1954); L. Van Hove, *Physica (Amsterdam)* **21**, 901 (1955); see also S. S. Schweber, *An Introduction to Relativistic Quantum Field Theory* (Row, Peterson, New York, 1961).
- [27] K. Huang, *Statistical Mechanics* (Wiley, New York, 1963).
- [28] K. Huang and C.N. Yang, *Phys. Rev.* **105**, 767 (1957); T.D. Lee, K. Huang, and C.N. Yang, *ibid.* **106**, 1135 (1957).
- [29] C.M. Caves and D.D. Crouch, *J. Opt. Soc. Am. B* **4**, 1535 (1987); M.G. Raymer, P.D. Drummond, and S.J. Carter, *Opt. Lett.* **16**, 1189 (1991); M. Hillery and L.D. Mlodinov, *Phys. Rev. A* **30**, 1860 (1984); P.D. Drummond, *ibid.* **42**, 6845 (1990).
- [30] A. A. Abrikosov, L. P. Gorkov, and I. E. Dzyaloshinski, *Methods of Quantum Field Theory in Statistical Physics* (Dover, New York, 1963); N.N. Bogolyubov, *J. Phys. (USSR)* **11**, 23 (1947); K.A. Brueckner and K. Sawada, *Phys. Rev.* **106**, 1117 (1957); K. Huang, C.N. Yang, and J.M. Luttinger, *ibid.* **105**, 776 (1957); N.P. Proukakis, K. Burnett, and H.T.C. Stoof, *Phys. Rev. A* **57**, 1230 (1998).
- [31] J.M. Vogels *et al.*, *Phys. Rev. A* **56**, R1067 (1997); P.S. Julienne *et al.*, *ibid.* **58**, R797 (1998); Y.B. Band and P.S. Julienne, *Phys. Rev. A* **51**, R4317 (1995); A. Vardi *et al.*, *J. Chem. Phys.* **107**, 6166 (1997); R. Côté and A. Dalgarno, *Chem. Phys. Lett.* **279**, 50 (1997).
- [32] N. Bloembergen, *Nonlinear Optics* (Benjamin, New York, 1965); P. N. Butcher and D. Cotter, *The Elements of Nonlinear Optics* (Cambridge University Press, Cambridge, 1990).
- [33] Z. Chen *et al.*, *Appl. Phys. Lett.* **61**, 2401 (1992); H. Xie, W.I. Wang, J.R. Meyer, and L.R. Ram-Mohan, *ibid.* **65**, 2048 (1994); M. Seto, *et al.*, *ibid.* **65**, 2969 (1994).
- [34] M.S. Wong, F. Pan, M. Bösch, R. Spreiter, C. Bosshard, P. Günter, and V. Gramlich, *J. Opt. Soc. Am. B* **15**, 426 (1998); R. Spreiter, C. Bosshard, G. Knöpfle, P. Günter, R.R. Tykwinski, M. Schreiber, and F. Diederich, *J. Phys. Chem. B* **102**, 29 (1998).
- [35] P. Tommasini, E. Timmermans, M. Hussein, and A. Kerman, cond-mat/9804015.
- [36] J. Javanainen and M. Mackie, *Phys. Rev. A* **59**, R3186 (1999).
- [37] S. Inouye *et al.*, *Nature (London)* **392**, 151 (1998); Ph. Courteille, R.S. Freeland, and D.J. Heinzen, *Phys. Rev. Lett.* **81**, 69 (1998).
- [38] J. Stenger, S. Inouye, M.R. Andrews, H.-J. Miesner, D.M. Stamper-Kurn, and W. Ketterle, *Phys. Rev. Lett.* **82**, 2422 (1999).
- [39] D. J. Heinzen (private communication); R.S. Freeland, R.H. Wynar, D.J. Han, and D.J. Heinzen, *Bull. Am. Phys. Soc.* **44**(1), 1007 (1999).
- [40] X. Liu, L.J. Qian, and F.W. Wise, *Phys. Rev. Lett.* **82**, 4631 (1999).
- [41] E. Timmermans, P. Tommasini, R. Côté, M. Hussein, and A. Kerman, e-print cond-mat/9805323; A.N. Salguero, M.C. Nemes, M.D. Sampaio, and A.F.R. de Toledo Piza, e-print quant-ph/9809003.
- [42] S.A. Morgan, R.J. Ballagh, and K. Burnett, *Phys. Rev. A* **55**, 4338 (1997); W.P. Reinhard and C.W. Clark, *J. Phys. B* **30**, L785 (1997); T.F. Scott, R.J. Ballagh, and K. Burnett, *ibid.* **31**, L329 (1998); O. Zobay, S. Pötting, P. Meystre, and E.M. Wright, *Phys. Rev. A* **59**, 643 (1999).